



HAL
open science

Distinct roles of forward and backward alpha-band waves in spatial visual attention

Andrea Alamia, Lucie Terral, Malo Renaud d'Ambra, Rufin Vanrullen

► **To cite this version:**

Andrea Alamia, Lucie Terral, Malo Renaud d'Ambra, Rufin Vanrullen. Distinct roles of forward and backward alpha-band waves in spatial visual attention. *eLife*, 2023, 12, 10.7554/eLife.85035 . hal-04025214

HAL Id: hal-04025214

<https://hal.science/hal-04025214>

Submitted on 12 Mar 2023

HAL is a multi-disciplinary open access archive for the deposit and dissemination of scientific research documents, whether they are published or not. The documents may come from teaching and research institutions in France or abroad, or from public or private research centers.

L'archive ouverte pluridisciplinaire **HAL**, est destinée au dépôt et à la diffusion de documents scientifiques de niveau recherche, publiés ou non, émanant des établissements d'enseignement et de recherche français ou étrangers, des laboratoires publics ou privés.

1 **Distinct roles of forward and backward alpha-band waves**
2 **in spatial visual attention**

3 Andrea Alamia^{1,2}, Lucie Terral¹, Malo Renaud D’Ambra¹ and Rufin VanRullen^{1,2}

4 ¹Cerco, CNRS Université de Toulouse, Toulouse 31052 (France)

5 ²Artificial and Natural Intelligence Toulouse Institute (ANITI), Toulouse (France)

6 andrea.alamia@cnrs.fr

7 Running title: *“Alpha-band traveling waves in visual attention”*

8

9

10

11

12

13

14

15

16

17

18

19

20

21

22

23

24

25

26

27

28

29

30

31

32

33 **Abstract (237/250)**

34 Previous research has associated alpha-band [8-12Hz] oscillations with inhibitory functions:
35 for instance, several studies showed that visual attention increases alpha-band power in the
36 hemisphere ipsilateral to the attended location. However, other studies demonstrated that
37 alpha oscillations positively correlate with visual perception, hinting at different processes
38 underlying their dynamics. Here, using an approach based on traveling waves, we
39 demonstrate that there are two functionally distinct alpha-band oscillations propagating in
40 different directions. We analyzed EEG recordings from three datasets of human participants
41 performing a covert visual attention task (one new dataset with N=16, two previously
42 published datasets with N=16 and N=31). Participants were instructed to detect a brief target
43 by covertly attending to the screen's left or right side. Our analysis reveals two distinct
44 processes: allocating attention to one hemifield increases top-down alpha-band waves
45 propagating from frontal to occipital regions ipsilateral to the attended location, both with or
46 without visual stimulation. These top-down oscillatory waves correlate positively with alpha-
47 band power in frontal and occipital regions. Yet, different alpha-band waves propagate from
48 occipital to frontal regions and contralateral to the attended location. Crucially, these forward
49 waves were present only during visual stimulation, suggesting a separate mechanism related
50 to visual processing. Together, these results reveal two distinct processes reflected by
51 different propagation directions, demonstrating the importance of considering oscillations as
52 traveling waves when characterizing their functional role.

53 **Keywords:** Traveling waves, covert visual attention, alpha-band oscillations, EEG recordings.

54

55

56

57

58

59

60

61

62

63 **Introduction**

64 Brain oscillations are related to several cognitive functions, as they orchestrate neuronal
65 activity at distinct temporal and spatial scales (Buzsáki and Draguhn, 2004; Buzsáki, 2009).
66 Alpha-band oscillations [8-12Hz] are the most prevailing rhythms in electrophysiological
67 (EEG) recordings, spreading through most cortical regions.

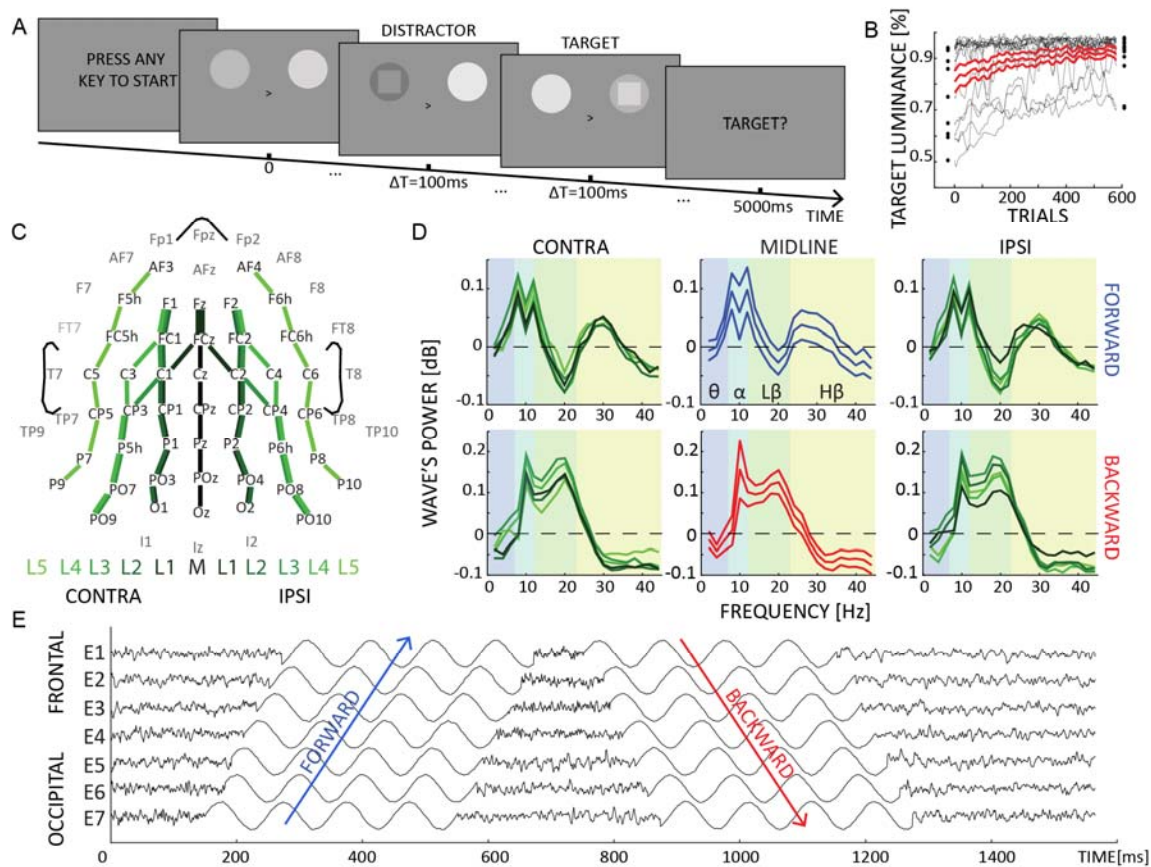
68 Several studies investigated their functional role in various cognitive processes (Palva and
69 Palva, 2007, 2011), providing mixed results. On the one hand, some studies showed that
70 alpha-band oscillations might filter sensory information, regulating excitation and inhibition
71 of sensory-specific brain regions (Jensen and Mazaheri, 2010; Mathewson et al., 2011;
72 Klimesch, 2012; Sadaghiani and Kleinschmidt, 2016). Accordingly, researchers interpreted
73 alpha oscillations as a top-down mechanism involved in inhibitory control and timing of
74 cortical processing (Klimesch et al., 2007), as well as modulating cortical excitability (Jensen
75 and Mazaheri, 2010; Mathewson et al., 2011). Experimental studies corroborated this
76 hypothesis, demonstrating how the phase of alpha-band oscillation affects visual perception
77 (Busch et al., 2009; Fakche et al., 2022; but see also Ruzzoli et al., 2019). Another highly
78 replicated result regarding the inhibitory role of alpha oscillations consists in the hemispheric
79 modulation in occipital regions associated with visual attention, having an increase of power
80 ipsilateral to the attended hemifield, and a corresponding decrease contralaterally (Worden et
81 al., 2000; Sauseng et al., 2005; Kelly et al., 2006; Thut et al., 2006; Händel et al., 2011). On
82 the other hand, other experimental studies have related alpha-band oscillations in occipital and
83 parietal regions to perceptual processing and visual memory (Bonnefond and Jensen, 2012;
84 VanRullen, 2016; Pang et al., 2020; Luo et al., 2021). For example, reverse-correlation
85 techniques reveal that the visual system reverberates sensory information in the alpha-band
86 for as long as one second, in what has been dubbed ‘perceptual echoes’ (Vanrullen and
87 MacDonald, 2012). Importantly, these echoes are a clear signature of sensory processing as
88 they reflect the input’s precise time course, are modulated by attention and have been
89 dissociated from inhibitory alpha power modulation (Vanrullen and MacDonald, 2012;
90 VanRullen, 2016; Brüers and VanRullen, 2018; Schwenk et al., 2020).

91 Altogether, these experimental evidences support distinct and contradictory conclusions about
92 alpha-band oscillation’s functional role(s), which remains an open debate. Here, we address
93 this question from a different perspective that interprets alpha-band oscillations as traveling
94 waves (Muller et al., 2018; Alamia and VanRullen, 2019), thus considering their spatial

95 component, and their propagation direction. Considering the case of visual attention, we
96 tested the hypothesis that two functionally distinct alpha-band oscillations propagate along the
97 frontal-occipital line in opposite directions. This compelling hypothesis about the different
98 functional roles of alpha-band traveling waves derives from our previous studies (Alamia and
99 VanRullen, 2019; Pang et al., 2020), in which we showed how visual perception modulates
100 alpha waves, i.e. forward waves during visual stimulation, backward waves when the stimulus
101 was off. In addition, this hypothesis is in line with previous studies suggesting that distinct
102 alpha-band oscillations are related to specific cognitive processes (Gulbinaite et al., 2017;
103 Deng et al., 2019; Schuhmann et al., 2019; Sokoliuk et al., 2019; Kasten et al., 2020). In this
104 study, we analyzed three datasets, two publicly available (Foster et al. 2017 and Feldmann-
105 Wustefeld et al. 2019, see below), and one collected specifically for this study. In all dataset,
106 participants attended either to the left or the right hemifield, while keeping central fixation.
107 Our results confirmed the hemispheric modulation of alpha-band oscillations in posterior
108 regions (Worden et al., 2000; Sauseng et al., 2005; Kelly et al., 2006; Thut et al., 2006;
109 Händel et al., 2011) and revealed two distinct alpha-band traveling waves propagating in
110 opposite directions. First, visual attention increases top-down alpha-band waves propagating
111 from frontal to occipital regions ipsilateral to the attended location, and such waves correlate
112 positively with alpha power in frontal and occipital regions. Moreover, our analysis
113 demonstrates that visual attention also modulates contralateral forward waves, i.e., waves
114 propagating from occipital to frontal areas. Importantly, the attentional modulation of forward
115 waves is crucially dependent on sustained sensory processing, as this modulation disappears
116 in the absence of visual stimulation. In contrast, alpha-band top-down waves are present and
117 modulated by visual attention irrespective of the presence or absence of concurrent sensory
118 stimulation. These results demonstrate two distinct alpha-band oscillatory waves propagating
119 in opposite directions, seemingly underlying different cognitive processes. The well-known
120 lateralization effect observed in alpha-band can be interpreted as top-down traveling waves,
121 and it's most likely related to inhibitory processes, in line with previous studies (Jensen and
122 Mazaheri, 2010; Händel et al., 2011). However, different alpha-band oscillations propagate in
123 a forward direction and are directly related to sensory processing, reconciling previous
124 evidence linking alpha-band oscillations with visual processing (Vanrullen and MacDonald,
125 2012; Lozano-Soldevilla and VanRullen, 2019).

126 **Results**

127 *Travelling waves' spectral profile.* The goal of the study was to investigate how
128 visual attention modulates alpha-band travelling waves in the hemisphere contra- and ipsi-
129 lateral to the attended location. To test this, we considered 11 lines of electrodes running from
130 occipital to frontal regions (figure 1C), 5 for each hemisphere and one midline. It is important
131 to note that the spatial resolution of these lines is not critical for our analysis, as we do not
132 expect significant differences within each hemisphere. However, before testing how visual
133 attention modulates travelling waves, we explored the amount of waves propagating forward
134 (FW) and backward (BW) as a function of their temporal frequency (see figure 5 and methods
135 for a detailed description of the analysis). Figure 1D shows the spectral profile of FW and BW
136 waves in the midline (along the Oz-Fz axis) and the contra- and ipsilateral lines: confirming
137 previous experimental studies (Alamia and VanRullen, 2019; Pang et al., 2020), we found that
138 alpha-band oscillatory waves propagate in both directions during visual stimulation, whereas
139 theta (4-7Hz) and high-beta/gamma (24-45Hz) bands propagate mostly bottom-up from
140 occipital to frontal regions, and low-beta (13-23Hz) waves flow in the top-down direction.
141 Interestingly, this pattern of results confirms previous studies using different methods, in
142 which higher frequency bands (i.e., high-beta/gamma) have been associated with forward
143 processing, whereas low-beta and alpha frequencies have been related to top-down
144 processing (Bastos et al., 2012, 2015; van Kerkoerle et al., 2014; Michalareas et al., 2016; but
145 see also Schneider et al., 2021).

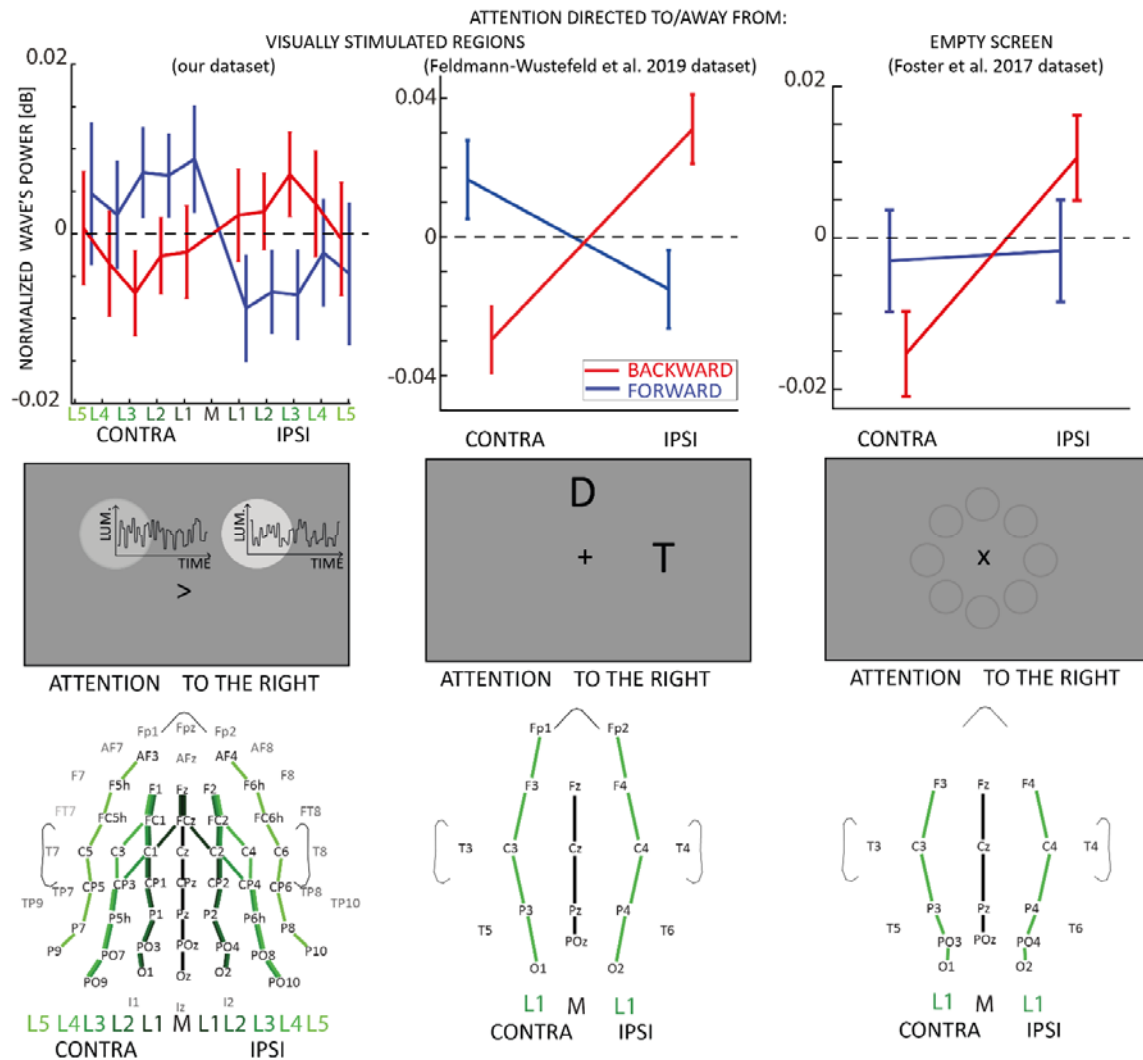


146

147 **Figure 1 – Experimental design and waves’ spectral profile.** A) Each trial lasted 5 seconds,
 148 in which two flickering stimuli were presented to both hemifield. Participants were instructed
 149 to attend either the left or the right hemifield, as indicated by a central cue. In some trials, a
 150 target or a distractor appeared for 100ms as a square either in the attended or unattended
 151 location. B) The target and distractor luminance changed over trials due to the QUEST
 152 algorithm, which kept participants’ performance around 80%. C) We quantified travelling
 153 waves along 11 electrodes lines, running along the anterior-posterior axis. These lines were
 154 located in the contralateral or the ipsilateral hemisphere to the attended location. D) The
 155 amount of waves in dB computed for forward (in blue) and backward (in red) waves in the
 156 midline (central subplots, thinner lines represent standard errors of the mean) and in the ipsi-
 157 and contralateral hemisphere (left and right panels, respectively). These waves were computed
 158 on trials without target or distractors. Positive (negative) values reflect more (less) waves than
 159 the chance level (as quantified by the surrogate distribution), whereas values around 0
 160 indicate no difference between the real and the null distribution. E) Simulated data providing
 161 a schematic representation of forward and backward waves in the time domain in a given line
 162 of electrodes (from more frontal E1 to more occipital E7). A positive and a negative phase
 163 shift characterized forward and backward waves, respectively.
 164

165 *Attending to visual stimuli modulates traveling waves.* In this analysis, we investigated
 166 how covert visual attention influences the traveling wave pattern. We focused on trials where
 167 neither a target nor a distractor was presented. First, we quantified the amount of traveling
 168 waves in the contra- and ipsi- lateral hemispheres to the attentional allocation. As shown in
 169 figure 2 (left column), we found a strong lateralization effect revealing an increase

170 (respectively, decrease) of contralateral (ipsilateral) forward waves in the alpha band, and the
 171 opposite pattern in waves propagating in the opposite direction. These results were confirmed
 172 by a Bayesian ANOVA, considering as factors DIRECTION (FW or BW), LINES (distance
 173 from the midline), and LATERALITY (contra vs ipsi). The results revealed strong evidence in
 174 favor of the interaction between DIRECTION and LATERALITY factors ($BF_{10}=31.230$,
 175 estimated error~1%, $\eta^2=0.08$ as estimated from a classical ANOVA), whereas all other
 176 factors and their interactions revealed evidence in favor of the absence of an effect
 177 ($BF_{s_{10}}<0.3$). We also found no significant effect in the other frequency bands (as shown in
 178 figure 1D, namely theta, low and high beta), hence we focused the following analyses on
 179 alpha-band oscillatory waves. These results demonstrate that the direction of alpha-band
 180 oscillatory traveling waves shows a laterality effect during a task involving covert selective
 181 attention.



182

183 **Figure 2 – Traveling waves block analysis.** Each column in the figure represents a different
 184 EEG dataset involving experiments with visual stimulation (left and middle column) and
 185 without visual stimulation (right column). In the upper panels, the net amount of forward
 186 (blue) and backward (red) waves is represented along different lines of electrodes, normalized
 187 to the midline. The left and central panels reveal an increase (decrease) of forward (backward)
 188 waves contralateral to the attended location when participants attended to visual stimulation.
 189 The right column shows that when participants attended an empty screen (data from Foster et
 190 al. 2017), only backward waves were modulated by visual attention, and no effect was
 191 observed in the forward waves without visual stimulation. Error bars represent standard errors
 192 of the mean. The middle row shows schematic representations of the screen during the tasks:
 193 the central panel illustrates the task from Feldmann-Wustefeld et al. 2019, where D and T
 194 stand for Distractor and Target, respectively. In the task from Foster et al. 2017, the screen
 195 was empty, as the eight circles were not displayed during the task but here illustrate the
 196 stimulus positions(Foster et al., 2017)(Foster et al., 2017). The lower panels represent the
 197 lines of electrodes in all datasets.

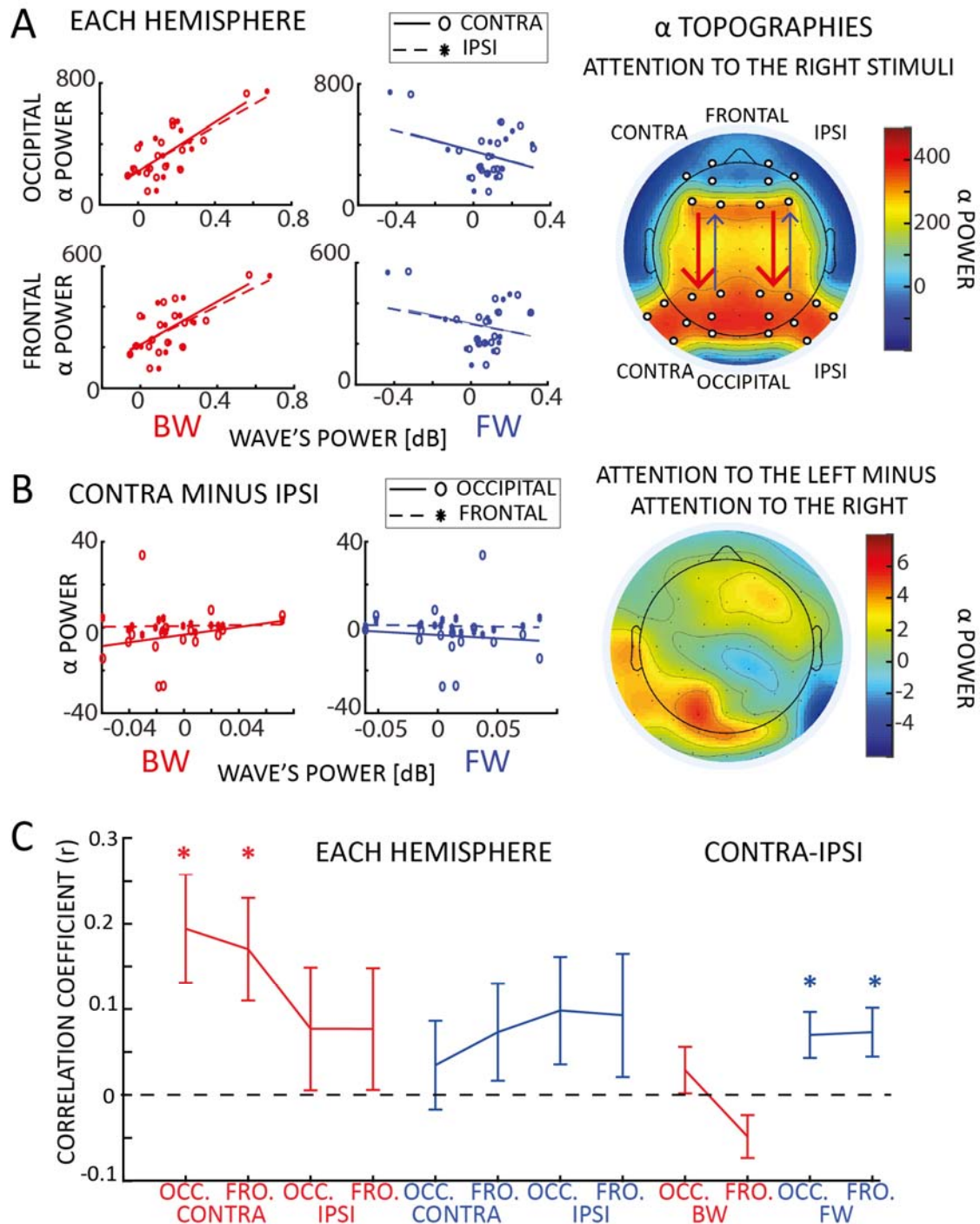
198 *Backward waves correlate with alpha-band power.* Previous studies investigating the
 199 role of alpha-band oscillations in visual attention reported a lateralization effect in the spectral
 200 power of alpha-band oscillations (Worden et al., 2000; Sauseng et al., 2005; Kelly et al.,
 201 2006; Thut et al., 2006; Jensen and Mazaheri, 2010; Händel et al., 2011). One may then
 202 wonder about the relationship between alpha power and traveling waves. To address this
 203 question, we investigated whether the oscillatory activity we observe propagating through the
 204 cortex relates to the spectral power in either occipital or frontal regions. We computed the
 205 averaged alpha-band power in frontal and occipital areas, contra- and ipsi- laterally to the
 206 target presentation, considering the same electrodes used for quantifying the traveling waves
 207 (see figure 3A). Interestingly, we found a significant positive correlation between alpha-band
 208 power in both occipital and frontal regions and backward waves, but not with forward waves
 209 (figure 3A – and Table 1). Next, we considered the lateralization effect in the alpha-band, as
 210 shown in figure 3B (topographic plot in the right panel) and well-replicated in previous
 211 studies (Sauseng et al., 2005; Thut et al., 2006; Händel et al., 2011). We wondered whether
 212 we could observe a correlation between such lateralization, defined as the difference between
 213 alpha-band power when attention is allocated to one side of the screen and to the other side,
 214 and the effect we reported in the travelling waves (figure 2). As shown in figure 3B (left
 215 panels), our results demonstrate a lack of correlation for both backward and forward waves in
 216 both frontal and occipital regions (all $|r| < 0.1$, $BF_{10} \sim 0.3$).

| Pearson r (BF ₁₀) | | FW | | BW | |
|----------------------------------|--------|----------------|----------------|-----------------------|-----------------------|
| | | CONTRA | IPSI | CONTRA | IPSI |
| ○ | CONTRA | -0.297 (0.549) | -0.350 (0.697) | 0.720 (28.519) | 0.698 (19.503) |

| | | | | | |
|-------|--------|----------------|----------------|------------------------|-----------------------|
| | IPSI | -0.305 (0.566) | -0.342 (0.669) | 0.786 (116.990) | 0.746 (47.512) |
| FRONT | CONTRA | -0.222 (0.422) | -0.252 (0.465) | 0.772 (84.225) | 0.712 (24.645) |
| | IPSI | -0.327 (0.625) | -0.354 (0.710) | 0.747 (48.448) | 0.705 (21.841) |

217 **Table 1 – Correlation with alpha-band power.** The table reports the Pearson
218 correlation coefficient and the Bayes Factor (BF_{10} supporting the alternative hypothesis, that
219 is the presence of a correlation) between frontal and occipital electrodes and forward (FW)
220 and backward (BW) waves, in both contralateral and ipsilateral hemisphere. All correlations
221 were computed on trials when neither a target nor a distractor was displayed.

222 To further investigate the relation between alpha-band travelling waves and alpha power, we
223 performed the same analysis focusing on the correlation within each participant. In particular,
224 we correlated trial-by-trial forward and backward waves with alpha-band power for each
225 subject, obtaining correlation coefficients ‘r’ and their respective p-values. As in the previous
226 analysis, we correlated forward and backward waves with frontal and occipital electrodes in
227 both contro- and ipsilateral hemispheres. We applied the Fisher method (Fisher, 1992, see
228 Methods for details) to combine all subjects' p-values in every conditions. Overall, we found a
229 significant effect of all combined p-values ($p < 0.0001$), except in the lateralization condition
230 (contra- minus ipsilateral hemisphere), similar to our previous analysis. Additionally, we
231 tested for a consistent positive or negative distribution of the correlation coefficients. As
232 shown in figure 3C, the results support a significant correlation between backward waves and
233 alpha-power in the hemisphere contralateral to the attended location ($BF_{10}=10.7$ and $BF_{10}=7.4$
234 for occipital and frontal regions, respectively; all other BF_{10} were between 1 and 2, providing
235 inconclusive evidence). Interestingly, this analysis also revealed a small but consistent effect
236 in the correlation between lateralization effects, as we reported a consistently positive
237 correlation in the contra- minus ipsilateral difference between forward waves and alpha power
238 ($BF_{10} \sim 5$ for both frontal and occipital electrodes). However, it's important to notice that the
239 combined p-values obtained using the Fisher method did not reach the significance threshold
240 in the lateralization condition, reducing the relevance of this specific result.



241

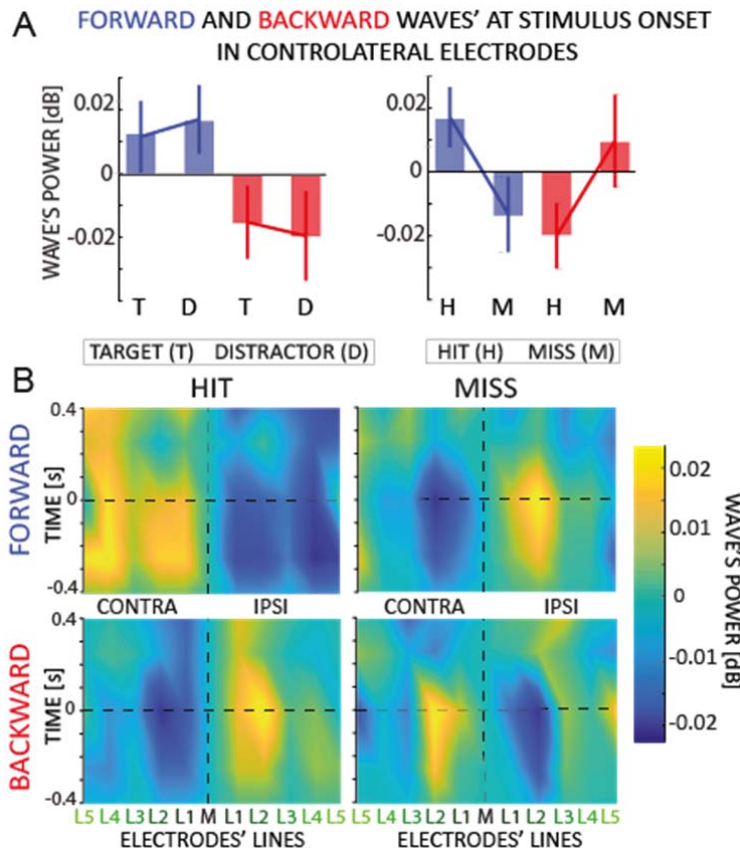
242 **Figure 3 - Correlation with alpha-band power.** A) Panel A reveals a correlation between
 243 backward waves and alpha power (static, standing power, i.e. measured via wavelets
 244 transform), in both frontal and occipital areas, in both hemispheres. We did not observe such
 245 correlation with forward waves. The plot to the right reveals the topographic distribution of
 246 alpha-power when participants attended to the right hemifield (we included the ‘left’
 247 condition by flipping the electrodes symmetrically to the midline). The white dots indicate the
 248 electrodes used for the correlation. B) The plots to the left show the correlation between the
 249 laterality effect in the alpha power and in the waves (laterality measured as the mean
 250 difference between contra and ipsilateral hemispheres for both alpha power and the waves –

251 for the waves we computed the difference using lines of electrodes symmetrical to the
252 midline). We did not observe any correlation in neither forward or backward waves, with
253 neither frontal or occipital alpha power. The topography to the right reveal a lateralization
254 effect in the alpha power (attention to the left minus attention to the right), confirming the
255 presence of alpha power lateralization, in line with previous studies (Sauseng et al., 2005;
256 Thut et al., 2006; Händel et al., 2011). C) Panel C shows the trial-by-trial correlation
257 coefficients averaged across participants for different conditions (as indicated in the x-axis).
258 Confirming the results in panel A, we found a positive correlation across participants between
259 backward waves and alpha-power, specifically in the contralateral hemisphere. We also
260 observed a positive global effect of the laterality condition across participants in the forward
261 waves, even though the combined p-values for the trial-by-trial correlation did not reach the
262 significant threshold.

263 *Covert attention modulates forward waves only with visual stimuli.* To confirm our
264 previous results, we replicated the same traveling waves analysis on two publicly available
265 EEG datasets in which participants performed similar attentional tasks (experiment 1 of
266 Foster et al., 2017 and experiment 1 of Feldmann-Wüstefeld and Vogel, 2019). In the first
267 experiment from the Feldmann-Wüstefeld and Vogel dataset, participants were instructed to
268 perform a visual working memory task in which, while keeping a central fixation, they had to
269 memorize a set of items while ignoring a group of distracting stimuli. We focused our
270 analysis on those trials in which the visual items to remember were placed either to the right
271 or the left side of the screen, while the distractors were either in the upper or lower part of the
272 screen (we pulled together the trials with either 2 or 4 distractors, as this factor was irrelevant
273 for our analysis). The stimuli were shown for 200ms, and we computed the amount of forward
274 and backward waves in the 500ms following stimulus onset. As shown in figure 2 (central
275 column), the analysis confirmed our previous results, demonstrating a strong interaction
276 between the factors DIRECTION and LATERALITY ($BF_{10}=667$, error~2%; independently, the
277 factors DIRECTION and LATERALITY had $BF_{10}=0.2$ and $BF_{10}=0.4$, respectively). These
278 results confirmed that spatial attention modulates both forward and backward waves in the
279 presence of visual stimulation. Next, we analyzed another publicly available dataset from
280 Foster et al., 2017. In the first experiment of Foster's study, participants completed a spatial
281 cueing task, requiring them to identify a digit among distractor letters. After a central cue was
282 displayed for 250ms, participants attended one of eight locations for 1000ms before the onset
283 of the target and distractors. As in our design, participants allocated attention to different
284 locations to the left or right of the screen while keeping central fixation. However, unlike in
285 our and in Feldmann-Wüstefeld's study, no stimulus was displayed while participants were
286 attending one of the possible locations. Here, we assessed the amount of waves in the 1000ms
287 before the onset of the stimulus during attention allocation, when no visual stimuli were

288 shown on the screen. Remarkably, as shown in figure 2 (right panel), our analysis
289 demonstrated an effect of the lateralization (LATERALITY: $BF_{10}=3.571$, error~1%), revealing
290 more waves contralateral to the attended location, but inconclusive results regarding the
291 interaction between DIRECTION and LATERALITY ($BF_{10}=2.056$, error~1%). However, using
292 a classical ANOVA (i.e., without modeling the slope of the random terms), the interaction
293 between DIRECTION and LATERALITY proved significant ($F(1,16)=9.81$, $p=0.003$, $\eta^2=0.13$).
294 In addition, when testing LATERALITY separately for forward and backward waves, we
295 observed an effect in the backward waves ($BF_{10}=3.497$, error<0.01%) but not in the forward
296 waves ($BF_{10}=0.231$, error<0.01%, supporting evidence in favor of the absence of an effect). In
297 addition, as analyzed in our dataset, we tested the correlation between backward waves and
298 alpha-band power in occipital (electrodes: PO3, PO4) and frontal (electrodes: F3, F4) regions.
299 We found moderate evidence of a positive correlation between contra- and ipsi- lateral
300 backward waves, and occipital (all Pearson's $r\sim 0.4$, all $BF_{S_{10}}\sim 3$) but inconclusive evidence
301 in the frontal areas (all Pearson's $r\sim 0.3$, all $BF_{S_{10}}\sim 2$). These results supported those from
302 our dataset, despite having a smaller amount of electrodes' lines, and potentially reduced
303 statistical power (see figure 2, lower panels). All in all, we could confirm our previous
304 conclusion that covert visual attention modulates top-down oscillatory waves, showing this
305 effect even in the absence of visual stimulation. In addition, we surmised that the
306 lateralization effect we reported in the forward waves in our dataset (absent in the Foster
307 dataset) is related to the steady visual stimulation during the attentional allocation, in line with
308 our previous results demonstrating that oscillatory bottom-up waves reflect sensory
309 processing (Alamia and VanRullen, 2019; Pang et al., 2020).

310 *Both detected targets and distractors elicit FW waves, but not missed targets.* In our
311 previous analysis, based on a subset of trials in which neither a target nor a distractor
312 occurred, we demonstrated that sustained attention to one hemifield generates oscillatory
313 alpha-band waves propagating forward in the contralateral hemisphere and backward in the
314 ipsilateral one. We now assess whether the occurrence of a specific event, such as the onset of
315 a target or a distractor stimulus, could induce the generation of transient oscillatory waves.
316 For this reason, we replicated the same analysis on those trials including either a target or a
317 distractor (on average, each participant performed 146.25 trials in each condition), to quantify
318 the amount of waves locked to the onset of these events.



319

320 **Figure 4 – Event analysis.** A) The figure shows the amount of forward (in blue) and
 321 backward (in red) contralateral waves around the onset of the target/distractor (left) or hit and
 322 missed targets (right panel). Error bars are standard error of the mean. We found an
 323 interaction effect when we analyzed the hit versus missed target. B) The 2D maps represent
 324 the amount of waves in the 11 lines of electrodes (x-axis) and around the onset time (y-axis)
 325 for forward and backward waves, and for hits and missed targets separately. The opposite
 326 pattern for hits vs. misses, already visible before the target onset, suggests that missed targets
 327 are due to a failure of attentional allocation rather than sensory processing; and consequently,
 328 that proper attentional allocation is characterized by contralateral forward waves and
 329 ipsilateral backward waves.
 330

331 The upper panels of figure 4A reveal the amount of forward and backward waves
 332 contralateral to the stimulus. Note that the targets and distractors appeared in the attended and
 333 unattended locations, respectively. A Bayesian ANOVA reveals no difference between targets
 334 and distractors (EVENT: $BF_{10}=0.206$, error~1%), or their interaction (DIRECTION x EVENT:
 335 $BF_{10}=0.423$, error~5%), as shown in the top-right panel of figure 4. This result reveals that
 336 both target and distractor elicit forward waves propagating contralateral to the hemifield
 337 where they occur. Next, we investigated whether the waves in the hemisphere contralateral to
 338 the attended hemifield correlate with the participant's performance in detecting the target (a
 339 QUEST algorithm kept the accuracy throughout the experiment around 80%). Remarkably,

340 we found an effect concerning the ‘hit’ and ‘miss’ target, as revealed by a significant
341 interaction of the DIRECTION and EVENT factors (DIRECTION x EVENT: $BF_{10}=4.085$,
342 error~2%), as shown in the bottom-right panel of figure 4A. Interestingly, figure 4B reveals
343 the amount of waves 400ms before and after the onset of the stimulus, showing how a missed
344 target is related to a decrease (increase) in forward (backward) waves contralateral
345 (ipsilateral) to the attended location, possibly due to attentional fluctuations during each trial.

346 **Discussion**

347 Previous studies demonstrated that selective attention modulates alpha-band oscillations in
348 occipital and parietal regions (Worden et al., 2000; Sauseng et al., 2005; Kelly et al., 2006;
349 Thut et al., 2006; Händel et al., 2011), supposedly indicating their involvement in top-down,
350 inhibitory functions. Here, we took a novel perspective on these results by interpreting
351 oscillations as traveling waves (Muller et al., 2018), thus considering their spatial component
352 on top of the temporal one. Our results revealed two distinct alpha-band waves propagating in
353 opposite directions: attention modulates oscillations traveling from occipital to frontal regions
354 only in the presence of visual stimulation, thus relating forward waves to visual processing
355 (Lozano-Soldevilla and VanRullen, 2019; Pang et al., 2020); whereas oscillations propagating
356 in the opposite, top-down direction were modulated by attention irrespective of the presence
357 or absence of concurrent visual stimulation; as in standard studies of alpha power
358 lateralization (Worden et al., 2000; Sauseng et al., 2005; Kelly et al., 2006; Thut et al., 2006;
359 Händel et al., 2011), this attentional modulation involved both an decrease of alpha waves
360 contralateral to the attended location, and an ipsilateral increase.

361 In line with previous studies (Gulbinaite et al., 2017; Deng et al., 2019; Schuhmann et
362 al., 2019; Sokoliuk et al., 2019; Kasten et al., 2020), our results support the thesis that distinct
363 alpha-band oscillations are involved in separate cognitive processes. A recent study from
364 Sokoliuk and colleagues (Sokoliuk et al., 2019) demonstrated two different sources of alpha-
365 band oscillations during a multisensory task: one, located in visual areas, reflects the
366 “spotlight of attention” and decreases linearly with increasing attention, whereas another one
367 indicates attentional efforts and occurs in parietal regions. Gulbinaite and colleagues also
368 demonstrated that parietal, but not occipital alpha-band oscillations are responsible for the
369 oscillatory reverberation causing the ‘triple-flash’ illusion (Gulbinaite et al., 2017). Similarly,
370 another study (Kasten et al., 2020) disentangled two primary sources of alpha oscillations,
371 revealing a differential effect of tACS stimulation on endogenous but not exogenous attention.
372 The authors interpreted their results as evidence supporting the hypothesis that alpha-band

373 oscillations play a causal role in top-down but not bottom-up attention (Schuhmann et al.,
374 2019; Kasten et al., 2020). Our results are consistent with these findings, including the spatial
375 dimension in analyzing and interpreting alpha-band oscillations. Additionally, we also found a
376 significant correlation between backward waves and occipital and frontal alpha-band power,
377 consistently with Kasten's study (Kasten et al., 2020) and the inhibitory role of alpha-band
378 oscillations. Our findings support the hypothesis that top-down processes, as reflected by
379 backward waves, drive the well-documented hemispheric asymmetries reported in the
380 literature (Händel et al., 2011; Klimesch, 2012; Waldhauser et al., 2012; Peylo et al., 2021).
381 All in all, previous studies and our results pave the way for a more comprehensive
382 understanding of the role of alpha-oscillations in cognition.

383 One may wonder whether alpha-band oscillations during attention relate to target
384 enhancement or distractor suppression (Schneider et al., 2021a). In the first case, the
385 desynchronization of alpha activity would favor the sensory processing in the hemisphere
386 contralateral to the target, whereas in the second case, alpha synchronization would suppress
387 the processing of the distractor (Kelly et al., 2006; Noonan et al., 2018; Peylo et al., 2021).
388 Our findings don't address this question directly but provide another element to the picture,
389 suggesting the intriguing hypothesis that target enhancement is not reflected in the alpha
390 power decrease but rather in an increase in the contralateral alpha-band waves processing the
391 target and propagating forward. Our results thus support the hypothesis that alpha waves are
392 involved in both distractor suppression (via ipsilateral top-down inhibitory feedback) and
393 target enhancement (via contralateral bottom-up alpha-band waves). Future studies will
394 precisely characterize the anatomical pathways of the distinct alpha-band oscillations,
395 possibly involving cortical dynamics in the ventral and dorsal streams (Capilla et al., 2014) or
396 cortico-thalamic connections (Lopes da Silva et al., 1980; Halgren et al., 2019).

397 Concerning the anatomical pathway of waves' propagation, our analysis based on
398 EEG recordings prevents us from clearly determining whether the observed waves propagate
399 through the cortex or whether more localized dipoles generate such widespread observations
400 at the sensor level. A previous source-analysis study on different visual-task datasets (Lozano-
401 Soldevilla and VanRullen, 2019) leaves both possibilities open. However, recent simulations
402 on perceptual echo data (related to bottom-up, sensory waves, Zhigalov and Jensen, 2022)
403 suggest that two dipoles in occipital and parietal regions could be responsible for the
404 generation of the waves propagating in the occipital-to-frontal direction. Supposing this
405 conclusion generalizes to raw EEG data and not only perceptual echoes (Vanrullen and
406 MacDonald, 2012), one could speculate that visual attention modulates dipoles selectively in

407 each hemisphere. However, one may wonder whether similar dipoles are also responsible for
408 generating top-down waves in frontal regions or whether other mechanisms are involved in
409 generating alpha-band backward waves.

410 Our previous work proposed an alternative cause for the generation of cortical waves
411 (Alamia and VanRullen, 2019). We demonstrated that a simple multi-level hierarchical model
412 based on Predictive Coding (PC) principles and implementing biologically plausible
413 constraints (temporal delays between brain areas and neural time constants) gives rise to
414 oscillatory traveling waves propagating both forward and backward. This model is also
415 consistent with the 2-dipoles hypothesis (Zhigalov and Jensen, 2022), considering the
416 interaction between the parietal and occipital areas (i.e., a model of 2 hierarchical levels).
417 However, dipoles in parietal regions are unlikely to explain the observed pattern of top-down
418 waves, suggesting that more frontal areas may be involved in generating the feedback. This
419 hypothesis is in line with the PC framework, in which top-down connections have an
420 inhibitory function, suppressing the activity predicted by higher-level regions (Huang and
421 Rao, 2011). Interestingly, Spratling proposed a simple reformulation of the terms in the PC
422 equations that could describe it as a model of biased competition in visual attention, thus
423 corroborating the interpretation of our finding within the PC framework (Spratling, 2008,
424 2012).

425 In conclusion, our study demonstrated the existence of two functionally distinct alpha-
426 band traveling waves propagating in opposite directions and modulated by visual attention.
427 Top-down waves prevail in the hemisphere ipsilateral to the attended location and are related
428 to inhibitory functions, whereas forward waves reflect ongoing visual processes in the
429 contralateral hemisphere.

430

431 **Methods**

432 **Participants.** EEG data were recorded from 16 volunteers (aged 20–32 years old, four
433 women, three left-handed). All subjects reported normal or corrected-to-normal vision, and
434 they had no history of epileptic seizures or photosensitivity. All participants gave written
435 informed consent before starting the experiment, following the Declaration of Helsinki. This
436 study adheres to the guidelines for research at the “Centre de Recherche Cerveau et
437 Cognition,” and the protocol was approved by the local ethical committee “Comité de
438 protection des Personnes Sud Méditerranée 1” (ethics approval number N° 2019-A02641-56).
439 Furthermore, we included EEG recordings from two additional publicly available datasets

440 investigating distinct scientific questions and using different analyses than our study. In the
441 first one, 31 participants performed a visual working memory task involving spatial attention.
442 The data were published in a previous study (Feldmann-Wüstefeld and Vogel, 2019, data
443 available online at <https://osf.io/a65xz/>). In the second dataset, 16 participants performed a
444 task involving covert spatial attention. These data were published in another study (Foster et
445 al., 2017, data available online at <https://osf.io/m64ue>). The number of participants in our
446 dataset was estimated based on a power analysis of previous studies investigating travelling
447 waves in vision (Luo et al., 2021) and to match the number of participant in the third dataset
448 (Foster et al., 2017). Our dataset is also available online at <https://osf.io/pn784/>.

449 **Experimental procedure.** The following describes the experimental procedure to
450 collect the data never published before. After setting the EEG device and placing the
451 electrodes, participants performed the task in a dim and quiet room. The experiment was
452 composed of 10 blocks of 60 trials each. During each trial (described in figure 1A), two
453 flickering luminance disks were displayed for 5 seconds, 9° to the left and right from the
454 center of the screen. The flicker had a frequency of 160Hz, and the intensities were pooled
455 from a uniform distribution. We chose to apply flickering stimulation to keep participants
456 engaged in the task and avoid attentional captures due to sudden target/distractor onset and
457 offset (see below). Before each block, participants were instructed to allocate attention to
458 either the right or the left stimulus while focusing on a central arrow located at the center of
459 the screen. The arrow pointed to the attended location and served as a visual reminder
460 throughout the block. In half of the trials, a target or a distractor flashed 100ms inside the
461 attended or non-attended stimulus (see figure 1A). Their onset could occur any time after the
462 first 500ms of the trial. Both target and distractor were squares whose luminance was a
463 percentage of the disk's luminance (i.e., when at 100%, targets/distractors were indiscernible
464 from the disk, as they have the same luminance). A QUEST algorithm (Watson and Pelli,
465 1983) modulated such percentage to keep participants' performance around 80% throughout
466 the experiment (see fig. 1B). In the other half of the trials, either the target followed the
467 distractor's onset, or neither the target nor the distractor was presented (in sum, four possible
468 trials occurred with the same frequency: either only a target, or only a distractor, or a target
469 preceded by a distractor, or neither of them). Participants reported whether they saw a target
470 only at each trial's end to prevent motor activity from confounding the EEG signals. All
471 stimuli were generated in MATLAB using the Psychtoolbox (Brainard, 1997).

472 We included two additional datasets in this study. In both studies, participants
473 performed a visual attention task while keeping their fixation in the center of the screen.

474 Regarding the Feldmann-Wüstefeld and Vogel, 2019 study, participants were asked to
475 memorize the colors of two stimuli while ignoring a set of distractors stimuli. We analyzed
476 uniquely those trials in which the visual stimuli were presented to the left or right side of the
477 screen, while the distractors were placed above or below the fixation cross. After 500ms of
478 the fixation cross, two colored ‘target’ stimuli were presented for 200ms. Participants were
479 asked to memorize these stimuli, and a new ‘probe’ stimulus was shown after an additional
480 second. Participants reported whether the probe matched the target stimuli or not. We
481 analyzed the traveling waves in the 500ms following the target stimulus onset.

482 Participants performed a spatial attention task in the second dataset from Foster et al.
483 2017. First, the fixation cross cued participants to covertly attend one of eight possible spatial
484 positions uniformly distributed around the center of the screen. After one second, a digit was
485 displayed either in the cued location or in any other one. The remaining locations were filled
486 with letters. Participants were instructed to report the displayed digit. We analyzed the waves
487 the second before the stimuli onset when participants were attending to the locations cued to
488 the left or right side of the screen (we discarded trials in which participants attended locations
489 above or below the fixation cross). For additional details about both experimental procedures,
490 we refer the reader to Foster et al., 2017 and Feldmann-Wüstefeld and Vogel, 2019.

491 **EEG recording and Preprocessing.** Throughout the experiment, we recorded EEG
492 signals using a 64-channel active BioSemi EEG system (1024Hz sampling rate), with three
493 additional ocular electrodes. The preprocessing consisted of down-sampling the data to 256Hz,
494 followed by a high-pass (>1Hz) and a notch (47-53Hz) filter. Data were then average-
495 referenced and segmented from 500ms before trial onset to its end. We performed the
496 preprocessing in EEGlab (Delorme and Makeig, 2004). Importantly, we carefully discarded
497 from all analyses all trials in which the EOG signals revealed eye movements.

498 **Traveling wave analysis.** As in our previous studies (Alamia et al., 2020; Pang et al.,
499 2020), we quantified traveling waves' propagation along eleven lines of seven electrodes,
500 running from occipital to frontal regions. As shown in figure 1C, we considered one midline
501 (Oz, POz, Pz, CPz, Cz, FCz, Fz) and five lines spreading through the left and right
502 hemispheres, symmetrically to the midline. The electrodes' choice overlapped and covered a
503 large portion of each hemisphere. For each set of seven electrodes, we created 2D maps by
504 sliding a 500ms time window over the EEG signals (having a 250ms overlap) and computing
505 2D-FFT representations of each map (figure 5B). Notably, the power in the lower and upper
506 quadrants quantifies the amount of waves propagating forward (FW - from occipital to frontal
507 electrodes) and backward (BW - from frontal to occipital), respectively (see figure 5A). Next,

508 we performed the same procedure after shuffling the electrodes to obtain a baseline with the
 509 same spectral power but without information about the amount of FW/BW waves (note in
 510 figure 1D that the surrogate distribution accounts for the typical $\frac{1}{f}$ power trend, as well as the
 511 alpha peak). Lastly, for each frequency in the range [2-45Hz], we extracted the maximum
 512 values in the 2D-FFT spectra in both the real (FW, BW) and the shuffled data (FW_{ss}, BW_{ss}),
 513 obtaining the waves' amount in decibel [dB] as:

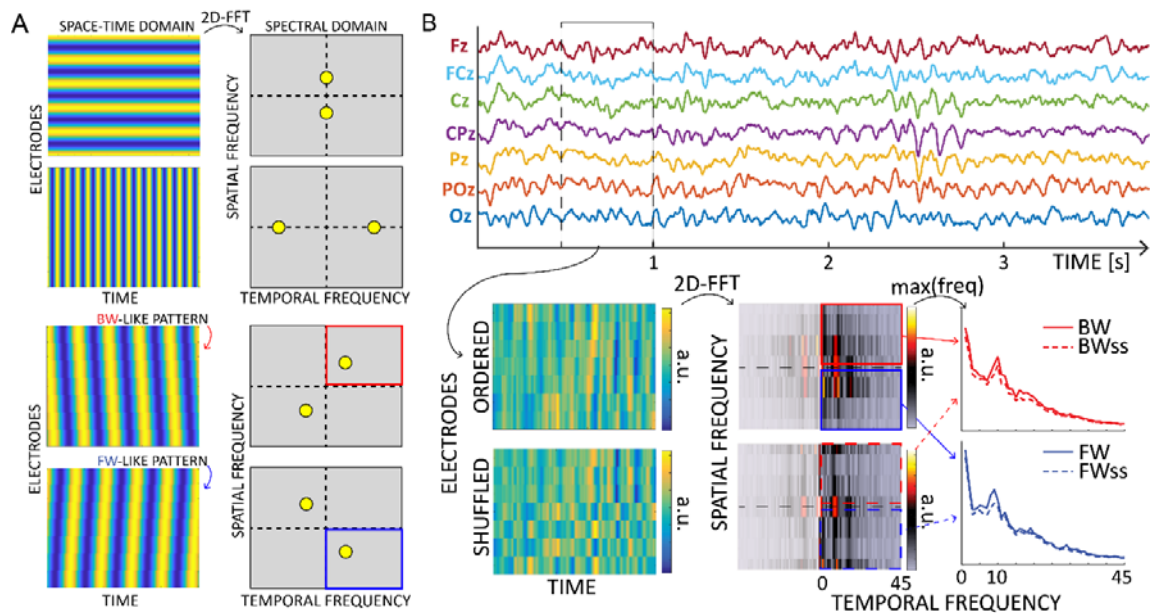
514

$$515 \quad FW \text{ waves [dB]} = 10 * \log_{10} \left(\frac{FW}{FW_{ss}} \right); \quad BW \text{ waves [dB]} = 10 * \log_{10} \left(\frac{BW}{BW_{ss}} \right).$$

516

517 This value quantifies the total waves compared to the null distribution, thus being
 518 informative when contrasted against zero. Importantly, this waves analysis is limited to the
 519 surface level, and does not directly inform about the underlying sources. It is also necessary to
 520 keep in mind issues related to long-range connections and distortions due to scalp interference
 521 (Nunez, 1974; Alexander et al., 2019).

522



523

524 **Figure 5 – Waves analysis.** A) The 2D-Fast Fourier Transform (2D-FFT) decomposes
 525 an image (e.g. a space-time representation of an EEG signal) into its spectral components. The
 526 upper part shows the decomposition of a 2D sinusoid propagating along the vertical or
 527 horizontal axis of the image. The corresponding peaks are found on the axis in the spectral
 528 domain, and their position depends on the frequency of the oscillations. The lower part of the
 529 figure show how the spectra change when the oscillations propagate with a backward- or
 530 forward- like pattern. Importantly, the spectral peaks rotate in two of the four quadrants
 531 depending on the direction, providing a reliable measure of forward or backward waves in the
 532 image. B) Schematic of the waves' quantification method. After defining time windows over
 each electrode line, we computed 2D Fourier transformation to quantify the amount of

533 forward (in blue) and backward (in red) waves. From the upper and lower quadrant of the 2D-
534 FFT spectra, we consider the maximum value over spatial frequencies, providing a 1D
535 spectrum of forward and backward waves in the temporal frequency domain. The same
536 procedure after shuffling the electrodes' order provides a surrogate measure, used as a
537 baseline. Notably, such surrogate distribution captures the 1/f trend and the alpha-band peak,
538 accounting for these factors in the final waves' quantification.

539
540 *Block analysis.* This analysis quantified the amount of traveling waves across all trials
541 when neither a target nor a distractor appeared. Participants paid attention to either one or the
542 other side of the screen, thus defining a contralateral and an ipsilateral hemisphere (see figure
543 1C). First, we averaged the forward and backward waves separately (in dB, see above) for
544 each map computed along the 11 lines of electrodes within the 5-second trial (five lines for
545 each hemisphere and the midline). Next, we averaged the results between trials, thus
546 obtaining five contra- and five ipsi- lateral spectra per subject for both FW and BW waves.
547 Although our hypothesis focuses on alpha-band oscillations, we also assessed the amount of
548 waves in other frequency bands. Accordingly, from each spectrum, we computed the average
549 per frequency band defined as θ (4-7Hz), α (8-12Hz), low β (13-24Hz) and high β/γ (25-
550 45Hz). Besides following the frequency band definition found in the literature, such division
551 reflects the waves' profile observed in the midline (fig.1D). Then, we normalized each pair of
552 symmetric lines (e.g., L1) by subtracting their mean value separately for each frequency band
553 (i.e., $\frac{L_{i, contra} + L_{i, ipsi}}{2}$). This normalization allows to remove power differences across lines
554 (e.g., L1, L2, etc.) and to compare the effects between hemispheres. Lastly, we tested an
555 ANOVA considering as factors DIRECTION (either FW or BW), LINE (a value from 1 to 5
556 to define the distance from the midline), LATERALITY (contra vs ipsi lateral), and all their
557 interactions. We considered SUBJECTS as the random factor in the model. All models in this
558 study relied on Bayesian statistics (see below for details). We performed the same analysis on
559 the EEG recordings from the second dataset (16 participants performing a similar attentional
560 task, see Foster et al., 2017, data available online at <https://osf.io/m64ue>). However, given the
561 available data, we were able to consider only one electrodes' line per hemisphere, using the
562 sensors O1-PO3-P3-C3-F3 and O2-PO4-P4-C4-F4 (see figure 2, lower left panel).

563 *Waves and power correlation.* This analysis assessed the correlation between FW and
564 BW waves computed in the block analysis, with occipital and frontal alpha power. First, we
565 estimated the mean alpha-power in contra- and ipsilateral electrodes in both frontal and
566 parieto-occipital regions, using the same electrodes involved in the waves' analysis (see figure
567 3B). We computed power spectra using wavelet transform (1-45Hz in log-space frequency
568 steps with 1-20 cycles) for all trials when neither a target nor a distractor appeared. We then

569 correlated the mean alpha power in both frontal and posterior regions with alpha-band
570 forward and backward waves between subjects in both contra and ipsilateral hemispheres. We
571 reported Bayes Factor and Pearson's coefficients. Additionally, we computed trial-by-trial
572 correlations between waves and alpha power for all participants. First, we tested the
573 correlation coefficient against zero in all conditions. Then, we obtained a combined p-value
574 per condition using the log/lin regress Fisher method (Fisher, 1992), as shown in (Zoefel et
575 al., 2019). Specifically, we computed the T value of a chi-square distribution with 2*N
576 degrees of freedom from the p_i values of the N participants as:

$$T = -2 * \sum_{i=1}^N \ln(p_i)$$

577 *Event analysis.* In this analysis, we first investigated how the onset of a target or a
578 distractor modulates the amount of both forward and backward waves, then whether a missed
579 or correctly identified target elicits different patterns of waves. In both cases, we performed
580 the same procedure as in the *block analysis*: we computed forward and backward waves
581 separately for each line of electrodes obtaining five contra- and five ipsilateral spectra per
582 subject. First, we computed the waves 500ms before and 500ms after the target or distractor's
583 onset, and we normalized each pair of symmetric lines as in the *block analysis* (see above).
584 Then, we tested two separate ANOVAs considering in the first analysis the factor EVENT
585 (either a target or a distractor occurred on the screen), and in the second the factor CORRECT
586 (either a hit or a missed target) in the second analysis. We included DIRECTION (either FW
587 or BW) in both models as a fixed factor and SUBJECTS as the random term.

588 **Statistical analyses.** We computed Bayes Factors (BF) in all statistical analyses,
589 measured as the ratio between the models testing the alternative against the null hypothesis.
590 All BFs follow this indication throughout the paper and are denoted as BF_{10} . Conventionally,
591 large BFs provide substantial ($BF > \sim 3$) or strong ($BF > \sim 10$) evidence in favor of the alternative
592 hypothesis, whereas low BF ($BF < \sim 0.333$) suggests a lack of effect (Smith, 2001; Masson,
593 2011). We performed all analyses in JASP (Love et al., 2015), considering default uniform
594 prior distributions. The code to analyze the travelling waves is freely available at the
595 following link: <https://github.com/artipago/Travelling-waves-EEG-2.0> (Alamia, 2023).

596

597 **Acknowledgments**

598 This work was funded by an ANR (OSCI-DEEP grant ANR-19-NEUC-0004) and ANITI
599 (Artificial and Natural Intelligence Toulouse Institute) Research Chair (grant ANR-19-PI3A-
600 0004) to R.V. A.A. has received funding from the European Research Council (ERC) under

601 the European Union's Horizon 2020 research and innovation program (grant agreement No
602 101075930)

603

604

605 **References**

- 606 Alamia A. (2023). Travelling-waves-EEG-2.0. <https://github.com/artipago/Travelling-waves-EEG-2.0>.
- 607 Alamia A, Timmermann C, Nutt DJ, Vanrullen R, Carhart-Harris RL (2020) DMT alters cortical travelling
608 waves. *Elife* 9:1–16.
- 609 Alamia A, VanRullen R (2019) Alpha oscillations and traveling waves: Signatures of predictive coding? *PLOS*
610 *Biol* 17:e3000487.
- 611 Alexander DM, Ball T, Schulze-Bonhage A, Van Leeuwen C (2019) Large-scale cortical travelling waves
612 predict localized future cortical signals. *PLoS Comput Biol* 15.
- 613 Bastos AM, Usrey WM, Adams RA, Mangun GR, Fries P, Friston KJ (2012) Canonical microcircuits for
614 predictive coding. *Neuron* 76:695–711 Available at:
615 [http://www.pubmedcentral.nih.gov/articlerender.fcgi?artid=3777738&tool=pmcentrez&rendertype=abstra](http://www.pubmedcentral.nih.gov/articlerender.fcgi?artid=3777738&tool=pmcentrez&rendertype=abstract)
616 [ct](http://www.pubmedcentral.nih.gov/articlerender.fcgi?artid=3777738&tool=pmcentrez&rendertype=abstract) [Accessed May 23, 2014].
- 617 Bastos AM, Vezoli J, Bosman CA, Schoffelen JM, Oostenveld R, Dowdall JR, DeWeerd P, Kennedy H, Fries P
618 (2015) Visual areas exert feedforward and feedback influences through distinct frequency channels.
619 *Neuron* 85:390–401.
- 620 Bonnefond M, Jensen O (2012) Alpha oscillations serve to protect working memory maintenance against
621 anticipated distracters. *Curr Biol* 22:1969–1974.
- 622 Brainard DH (1997) The Psychophysics Toolbox. *Spat Vis* 10:433–436 Available at:
623 <http://www.ncbi.nlm.nih.gov/pubmed/9176952>.
- 624 Brüers S, VanRullen R (2018) Alpha power modulates perception independently of endogenous factors. *Front*
625 *Neurosci* 12.
- 626 Busch NA, Dubois J, VanRullen R (2009) The phase of ongoing EEG oscillations predicts visual perception. *J*
627 *Neurosci* 29:7869–7876.
- 628 Buzsáki G (2009) *Rhythms of the Brain*. Oxford University Press.
- 629 Buzsáki G, Draguhn A (2004) Neuronal oscillations in cortical networks. *Science* (80-) 304:1926–1929.
- 630 Capilla A, Schoffelen JM, Paterson G, Thut G, Gross J (2014) Dissociated α -band modulations in the dorsal and
631 ventral visual pathways in visuospatial attention and perception. *Cereb Cortex*.
- 632 Delorme A, Makeig S (2004) EEGLAB: An open source toolbox for analysis of single-trial EEG dynamics
633 including independent component analysis. *J Neurosci Methods* 134:9–21.
- 634 Deng Y, Reinhart RMG, Choi I, Shinn-Cunningham B (2019) Causal links between parietal alpha activity and
635 spatial auditory attention. *Elife*.
- 636 Fakche C, Vanrullen R, Marque P, Dugué L (2022) α Phase-Amplitude Tradeoffs Predict Visual Perception.
637 *eNeuro* 9.
- 638 Feldmann-Wüstefeld T, Vogel EK (2019) Neural Evidence for the Contribution of Active Suppression During
639 Working Memory Filtering. *Cereb Cortex*.
- 640 Fisher RA (1992) *Statistical Methods for Research Workers*.

641 Foster JJ, Sutterer DW, Serences JT, Vogel EK, Awh E (2017) Alpha-Band Oscillations Enable Spatially and
642 Temporally Resolved Tracking of Covert Spatial Attention. *Psychol Sci* 28:929–941.

643 Gulbinaite R, İlhan B, Vanrullen R (2017) The triple-flash illusion reveals a driving role of alpha-band
644 reverberations in visual perception. *J Neurosci* 37:7219–7230.

645 Halgren M, Ulbert I, Bastuji H, Fabó D, Eross L, Rey M, Devinsky O, Doyle WK, Mak-McCully R, Halgren E,
646 Wittner L, Chauvel P, Heit G, Eskandar E, Mandell A, Cash SS (2019) The generation and propagation of
647 the human alpha rhythm. *Proc Natl Acad Sci U S A* 116:23772–23782.

648 Händel BF, Haarmeier T, Jensen O (2011) Alpha oscillations correlate with the successful inhibition of
649 unattended stimuli. *J Cogn Neurosci* 23:2494–2502.

650 Huang Y, Rao RPN (2011) Predictive coding. *Wiley Interdiscip Rev Cogn Sci* 2:580–593 Available at:
651 <http://doi.wiley.com/10.1002/wcs.142> [Accessed May 24, 2014].

652 Jensen O, Mazaheri A (2010) Shaping functional architecture by oscillatory alpha activity: Gating by inhibition.
653 *Front Hum Neurosci* 4 Available at:
654 <http://journal.frontiersin.org/article/10.3389/fnhum.2010.00186/abstract>.

655 Kasten FH, Wendeln T, Stecher HI, Herrmann CS (2020) Hemisphere-specific, differential effects of lateralized,
656 occipital–parietal α - versus γ -tACS on endogenous but not exogenous visual-spatial attention. *Sci Rep* 10.

657 Kelly SP, Lalor EC, Reilly RB, Foxe JJ (2006) Increases in alpha oscillatory power reflect an active retinotopic
658 mechanism for distracter suppression during sustained visuospatial attention. *J Neurophysiol* 95:3844–
659 3851.

660 Klimesch W (2012) Alpha-band oscillations, attention, and controlled access to stored information. *Trends Cogn*
661 *Sci* 16:606–617.

662 Klimesch W, Sauseng P, Hanslmayr S (2007) EEG alpha oscillations: The inhibition-timing hypothesis. *Brain*
663 *Res Rev* 53:63–88.

664 Lopes da Silva FH, Vos JE, Mooibroek J, van Rotterdam A (1980) Relative contributions of intracortical and
665 thalamo-cortical processes in the generation of alpha rhythms, revealed by partial coherence analysis.
666 *Electroencephalogr Clin Neurophysiol* 50:449–456.

667 Love J, Selker R, Verhagen J, Marsman M, Gronau QF, Jamil T, Smira M, Epskamp S, Wild A, Ly A, Matzke D,
668 Wagenmakers E-J, Morey RD, Rouder JN (2015) Software to sharpen your stats. *APS Obs* 28:27–29.

669 Lozano-Soldevilla D, VanRullen R (2019) The Hidden Spatial Dimension of Alpha: 10-Hz Perceptual Echoes
670 Propagate as Periodic Traveling Waves in the Human Brain. *Cell Rep* 26:374-380.e4 Available at:
671 <https://doi.org/10.1016/j.celrep.2018.12.058>.

672 Luo C, VanRullen R, Alamia A (2021) Conscious perception and perceptual echoes: a binocular rivalry study.
673 *Neurosci Conscious* 2021.

674 Masson MEJ (2011) A tutorial on a practical Bayesian alternative to null-hypothesis significance testing. :679–
675 690.

676 Mathewson KE, Lleras A, Beck DM, Fabiani M, Ro T, Gratton G (2011) Pulsed out of awareness: EEG alpha
677 oscillations represent a pulsed-inhibition of ongoing cortical processing. *Front Psychol* 2.

678 Michalareas G, Vezoli J, van Pelt S, Schoffelen JM, Kennedy H, Fries P (2016) Alpha-Beta and Gamma
679 Rhythms Subserve Feedback and Feedforward Influences among Human Visual Cortical Areas. *Neuron*
680 89:384–397.

681 Muller L, Chavane F, Reynolds J, Sejnowski TJ (2018) Cortical travelling waves: Mechanisms and
682 computational principles. *Nat Rev Neurosci* 19:255–268.

683 Noonan MAP, Crittenden BM, Jensen O, Stokes MG (2018) Selective inhibition of distracting input. *Behav*
684 *Brain Res.*

685 Nunez PL (1974) The brain wave equation: a model for the EEG. *Math Biosci* 21:279–297.

686 Palva S, Palva JM (2007) New vistas for α -frequency band oscillations. *Trends Neurosci* 30:150–158.

687 Palva S, Palva JM (2011) Functional roles of alpha-band phase synchronization in local and large-scale cortical
688 networks. *Front Psychol* 2.

689 Pang Z, Alamia A, Vanrullen R (2020) Turning the stimulus on and off changes the direction of α traveling
690 waves. *eNeuro* 7:1–11.

691 Peylo C, Hilla Y, Sauseng P (2021) Cause or consequence? Alpha oscillations in visuospatial attention. *Trends*
692 *Neurosci* 44:705–713.

693 Ruzzoli M, Torralba M, Moris Fernández L, Soto-Faraco S (2019) The relevance of alpha phase in human
694 perception. *Cortex* 120:249–268.

695 Sadaghiani S, Kleinschmidt A (2016) Brain Networks and α -Oscillations: Structural and Functional Foundations
696 of Cognitive Control. *Trends Cogn Sci.*

697 Sauseng P, Klimesch W, Stadler W, Schabus M, Doppelmayr M, Hanslmayr S, Gruber WR, Birbaumer N (2005)
698 A shift of visual spatial attention is selectively associated with human EEG alpha activity. *Eur J Neurosci*
699 22:2917–2926.

700 Schneider D, Herbst SK, Klatt LI, Wöstmann M (2021a) Target enhancement or distractor suppression?
701 Functionally distinct alpha oscillations form the basis of attention. *Eur J Neurosci.*

702 Schneider M, Broggin AC, Dann B, Tzanou A, Uran C, Sheshadri S, Scherberger H, Vinck M (2021b) A
703 mechanism for inter-areal coherence through communication based on connectivity and oscillatory power.
704 *Neuron* 109:4050-4067.e12.

705 Schuhmann T, Kemmerer SK, Duecker F, de Graaf TA, Oever S ten, de Weerd P, Sack AT (2019) Left parietal
706 tACS at alpha frequency induces a shift of visuospatial attention. *PLoS One* 14.

707 Schwenk JCB, VanRullen R, Bremmer F (2020) Dynamics of visual perceptual echoes following short-term
708 visual deprivation. *Cereb Cortex Commun.*

709 Smith JMB and AFM (2001) Bayesian Theory. *Meas Sci Technol* 12:221–222.

710 Sokoliuk R, Mayhew SD, Aquino KM, Wilson R, Brookes MJ, Francis ST, Hanslmayr S, Mullinger KJ (2019)
711 Two spatially distinct posterior alpha sources fulfill different functional roles in attention. *J Neurosci*
712 39:7183–7194.

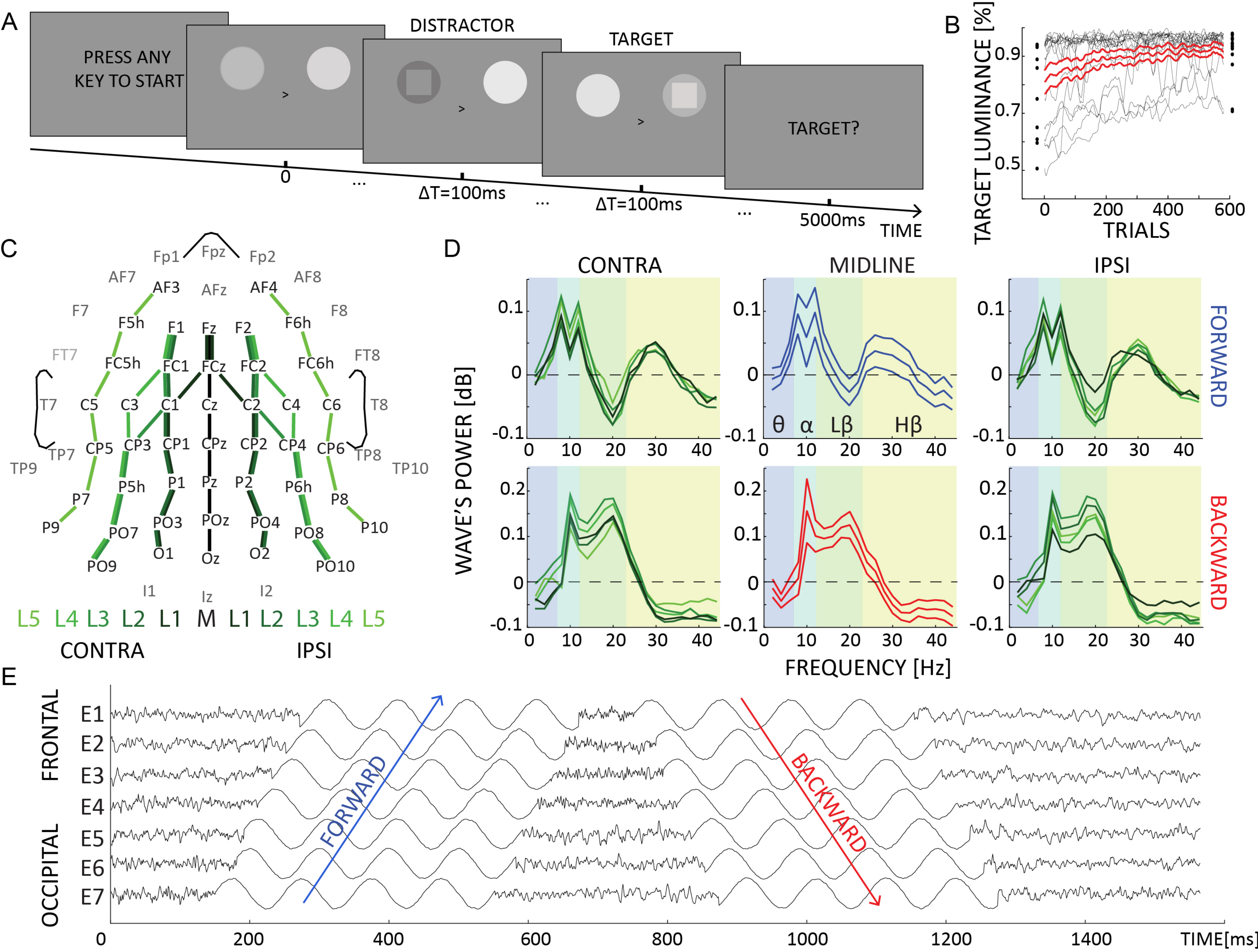
713 Spratling MW (2008) Predictive coding as a model of biased competition in visual attention. *Vision Res*
714 48:1391–1408.

715 Spratling MW (2012) Predictive coding as a model of the V1 saliency map hypothesis. *Neural Networks* 26:7–
716 28.

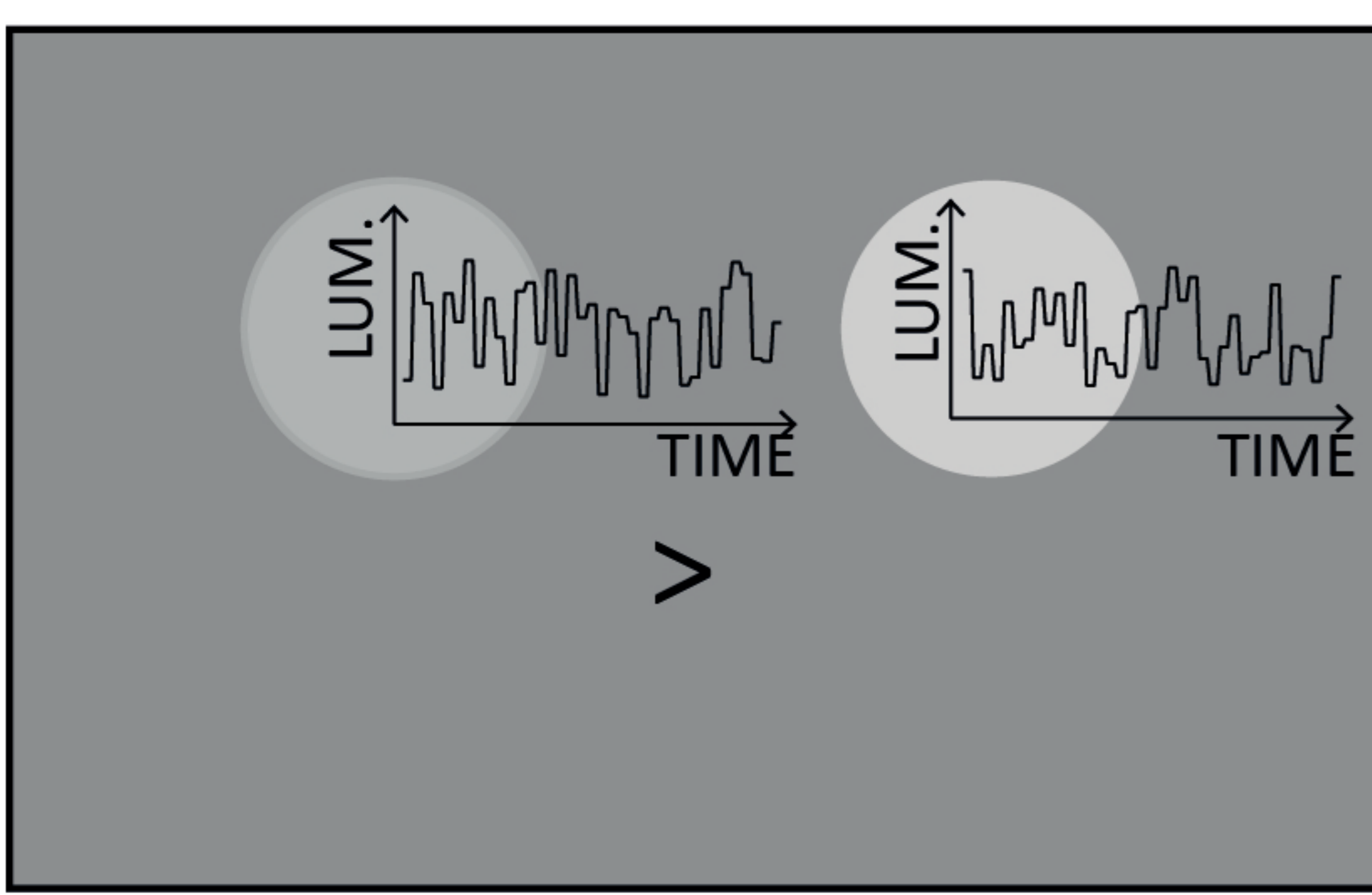
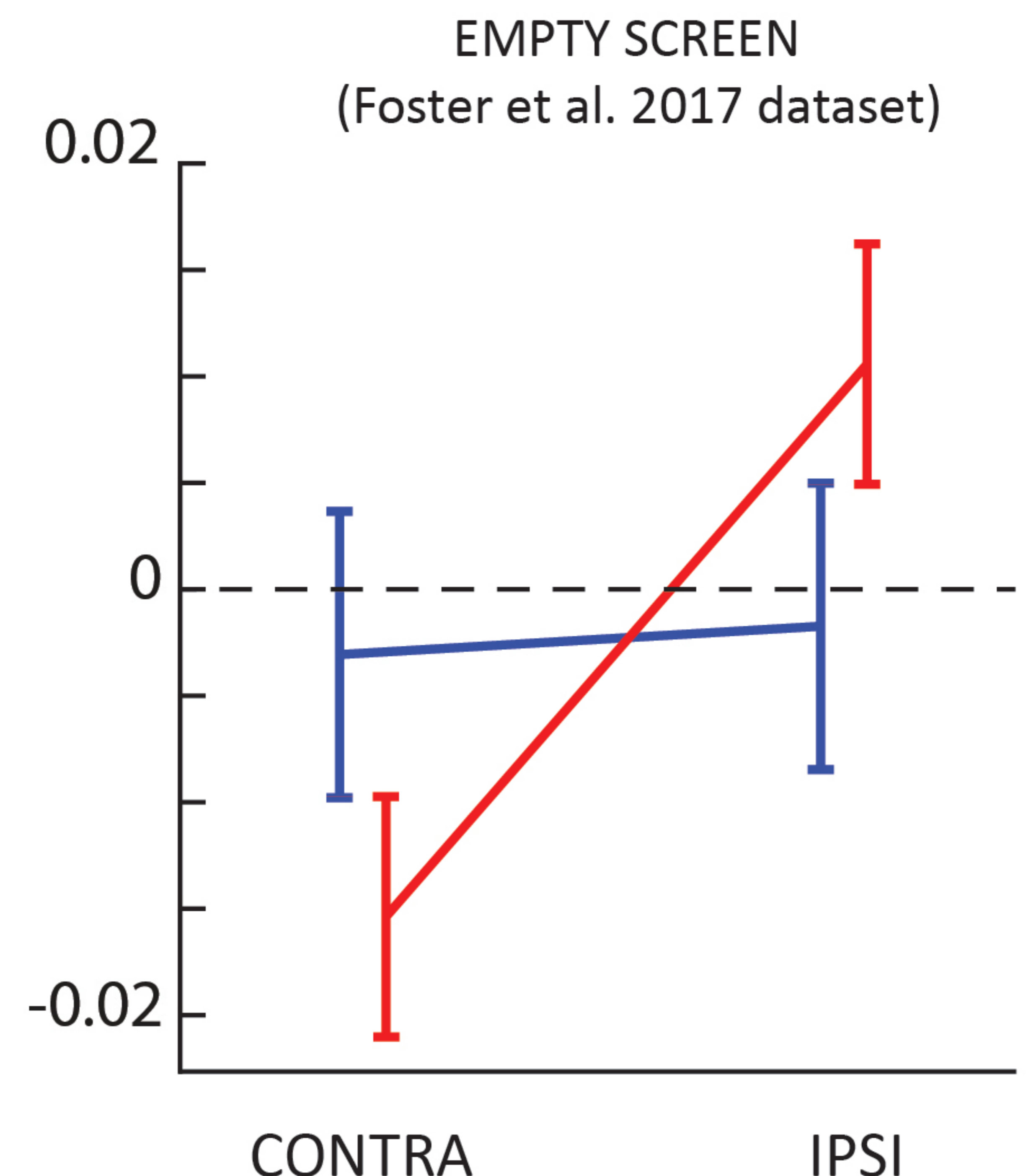
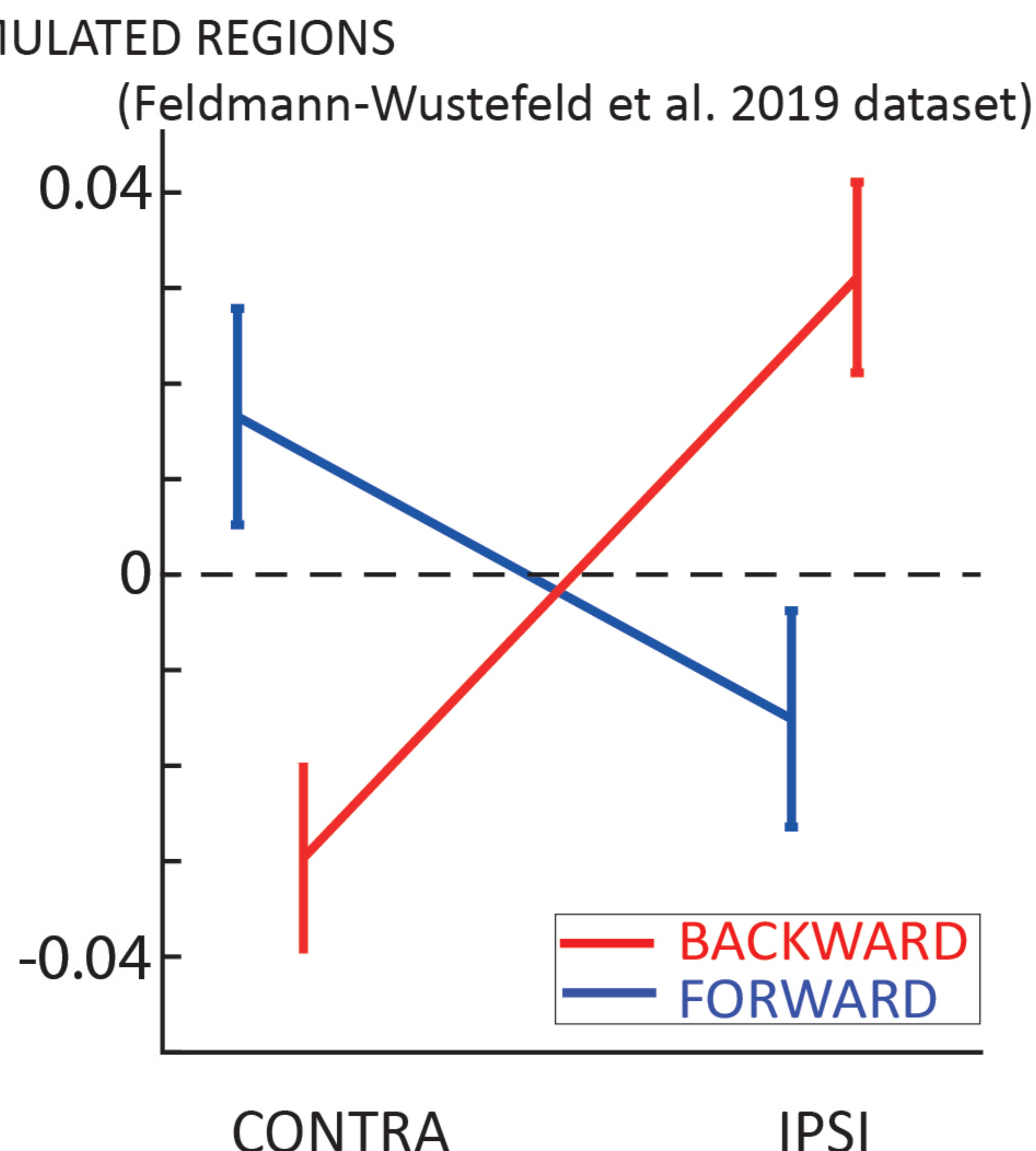
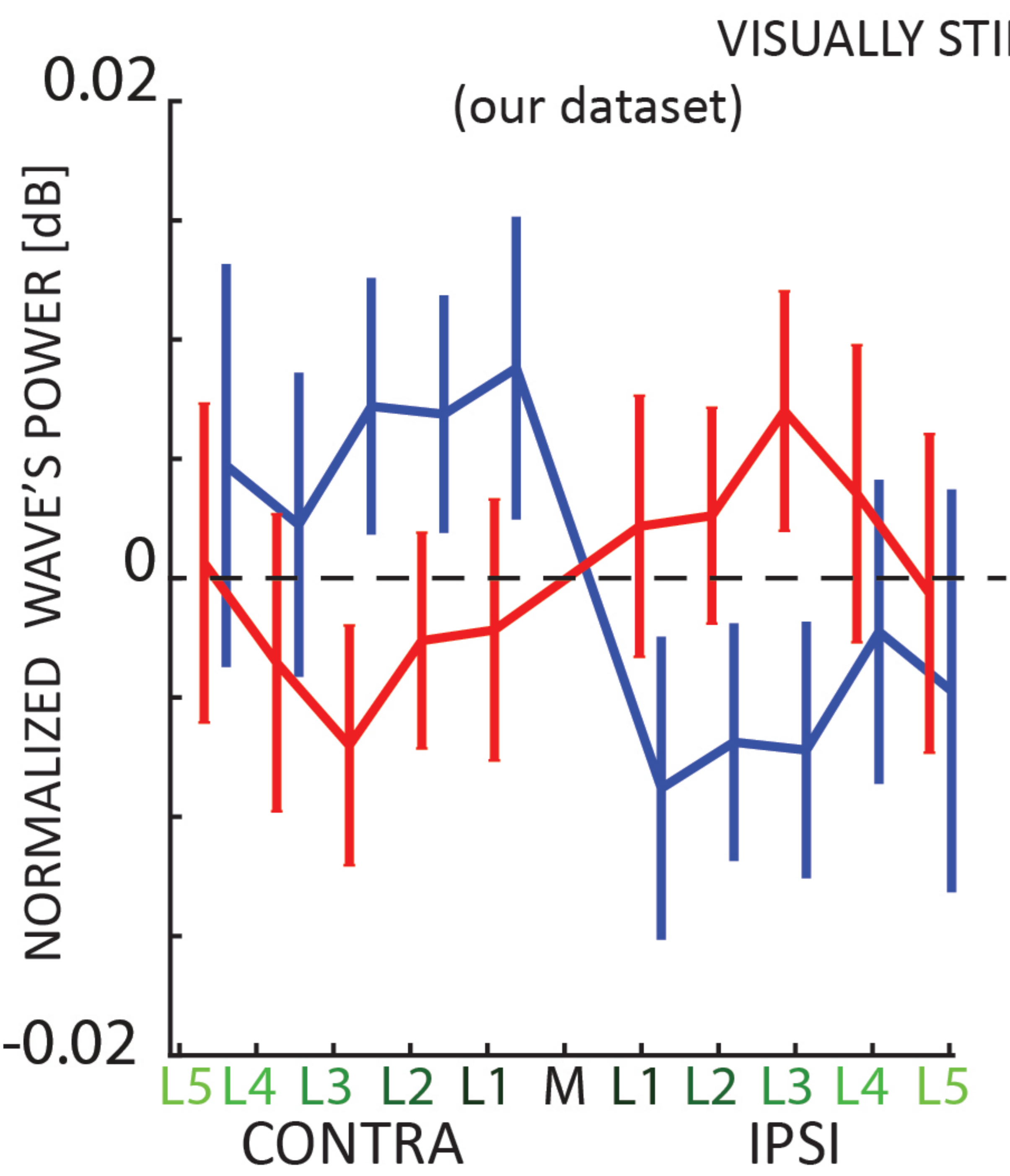
717 Thut G, Nietzel A, Brandt SA, Pascual-Leone A (2006) α -Band electroencephalographic activity over occipital
718 cortex indexes visuospatial attention bias and predicts visual target detection. *J Neurosci* 26:9494–9502.

719 van Kerkoerle T, Self MW, Dagnino B, Gariel-Mathis M-A, Poort J, van der Togt C, Roelfsema PR (2014)
720 Alpha and gamma oscillations characterize feedback and feedforward processing in monkey visual cortex.

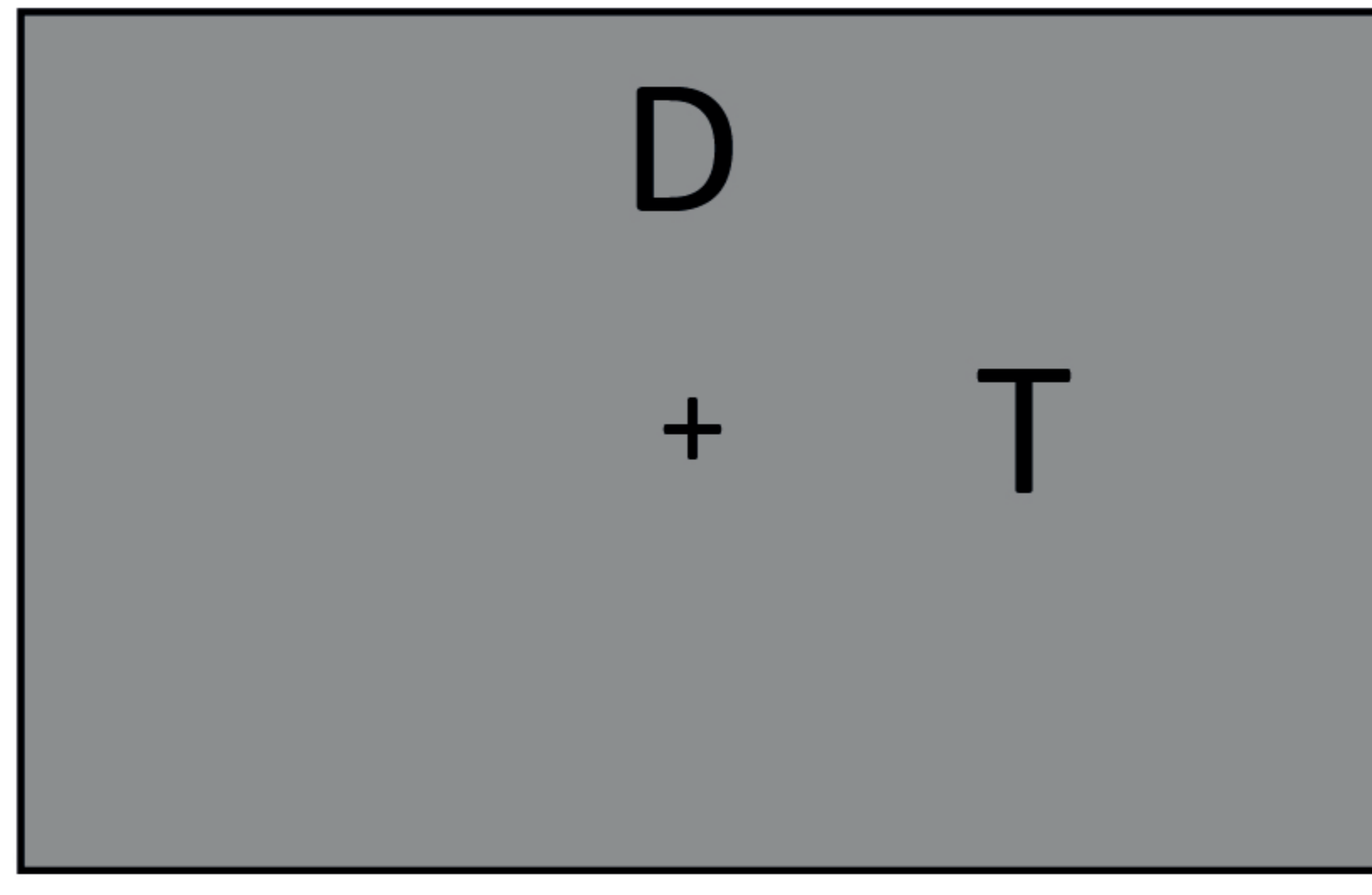
721 Proc Natl Acad Sci 111:14332–14341 Available at:
722 <http://www.pnas.org/lookup/doi/10.1073/pnas.1402773111>.
723 VanRullen R (2016) Perceptual Cycles. *Trends Cogn Sci* 20:723–735.
724 Vanrullen R, MacDonald JSP (2012) Perceptual echoes at 10 Hz in the human brain. *Curr Biol* 22:995–999.
725 Waldhauser GT, Johansson M, Hanslmayr S (2012) Alpha/Beta Oscillations Indicate Inhibition of Interfering
726 Visual Memories. *J Neurosci* 32:1953–1961.
727 Watson AB, Pelli DG (1983) Quest: A Bayesian adaptive psychometric method. *Percept Psychophys* 33:113–
728 120.
729 Worden MS, Foxe JJ, Wang N, Simpson G V. (2000) Anticipatory biasing of visuospatial attention indexed by
730 retinotopically specific alpha-band electroencephalography increases over occipital cortex. *J Neurosci* 20.
731 Zhigalov A, Jensen O (2022) Travelling waves observed in MEG data can be explained by two discrete sources.
732 bioarxiv Available at: <https://www.biorxiv.org/content/10.1101/2022.09.28.509870v2.abstract>.
733 Zoefel B, Davis MH, Valente G, Riecke L (2019) How to test for phasic modulation of neural and behavioural
734 responses. *Neuroimage*.
735



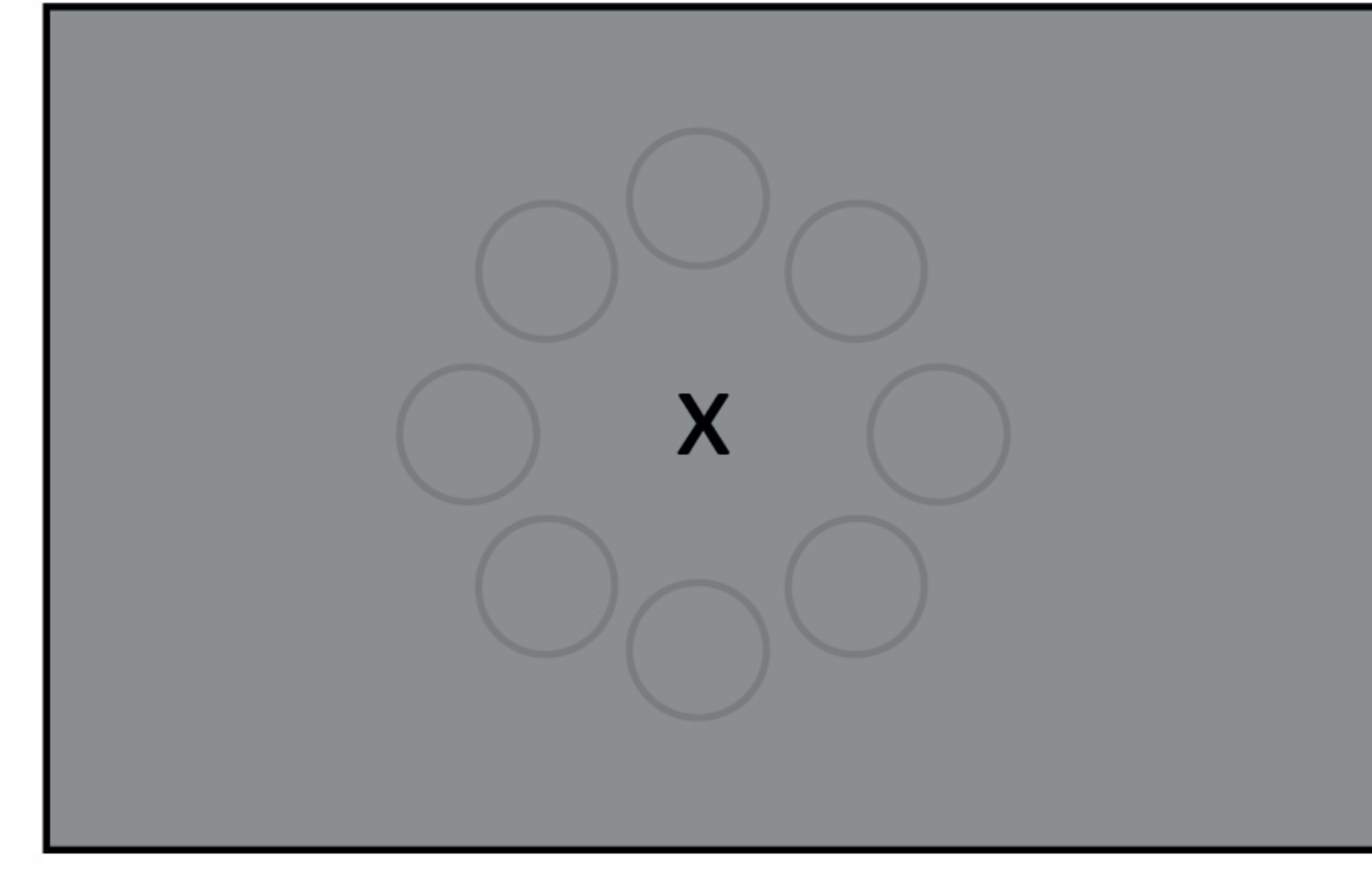
ATTENTION DIRECTED TO/AWAY FROM:



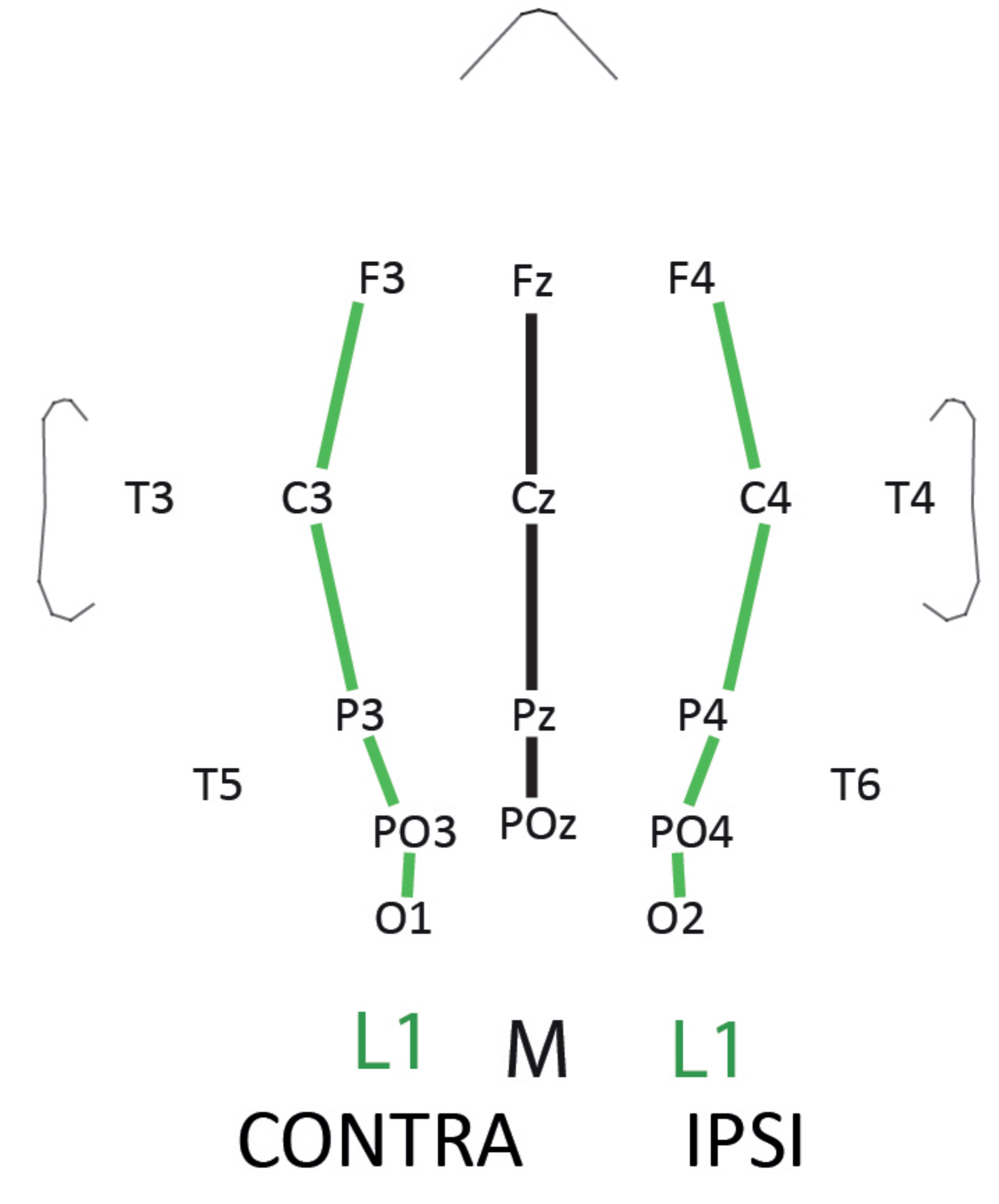
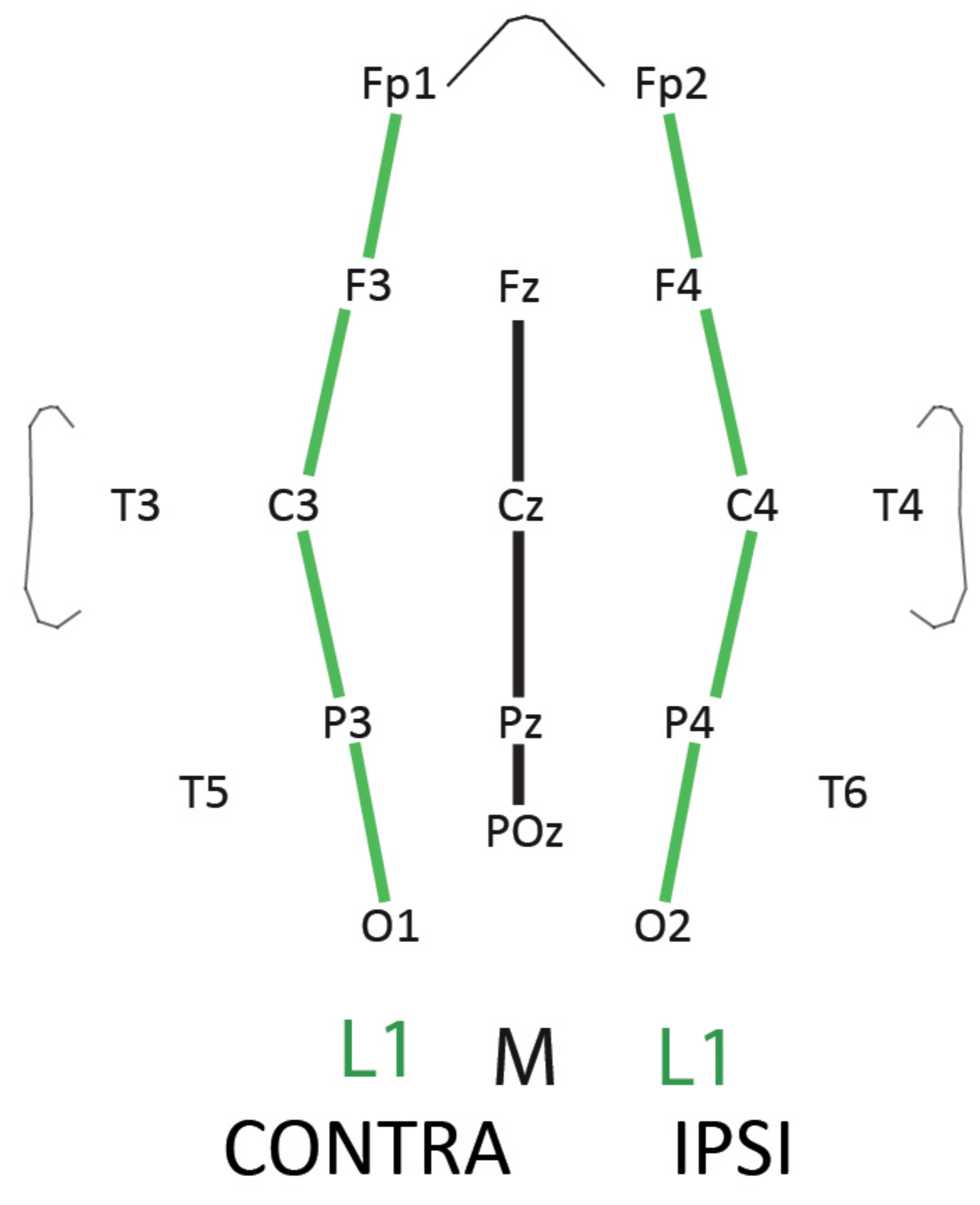
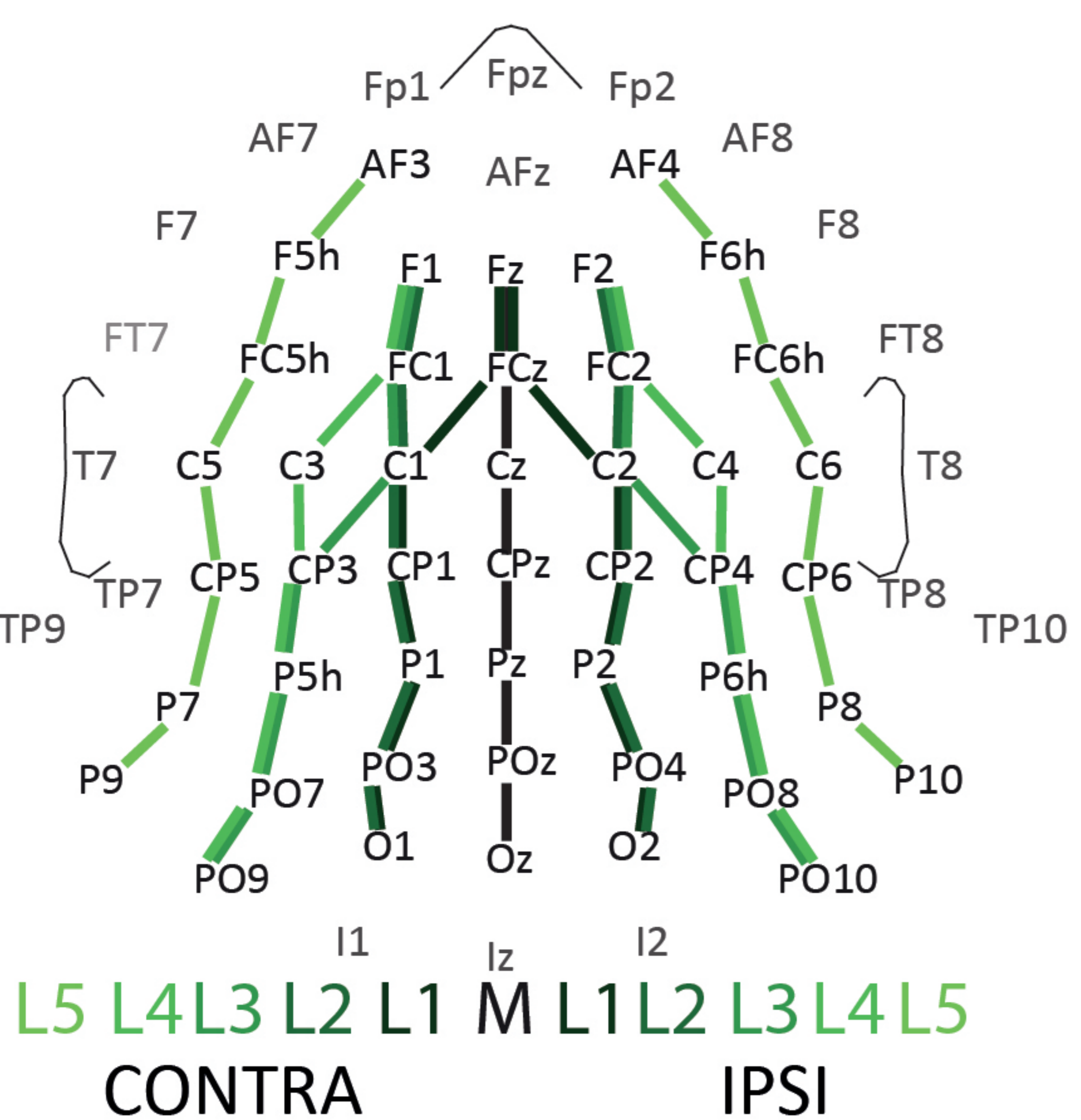
ATTENTION TO THE RIGHT

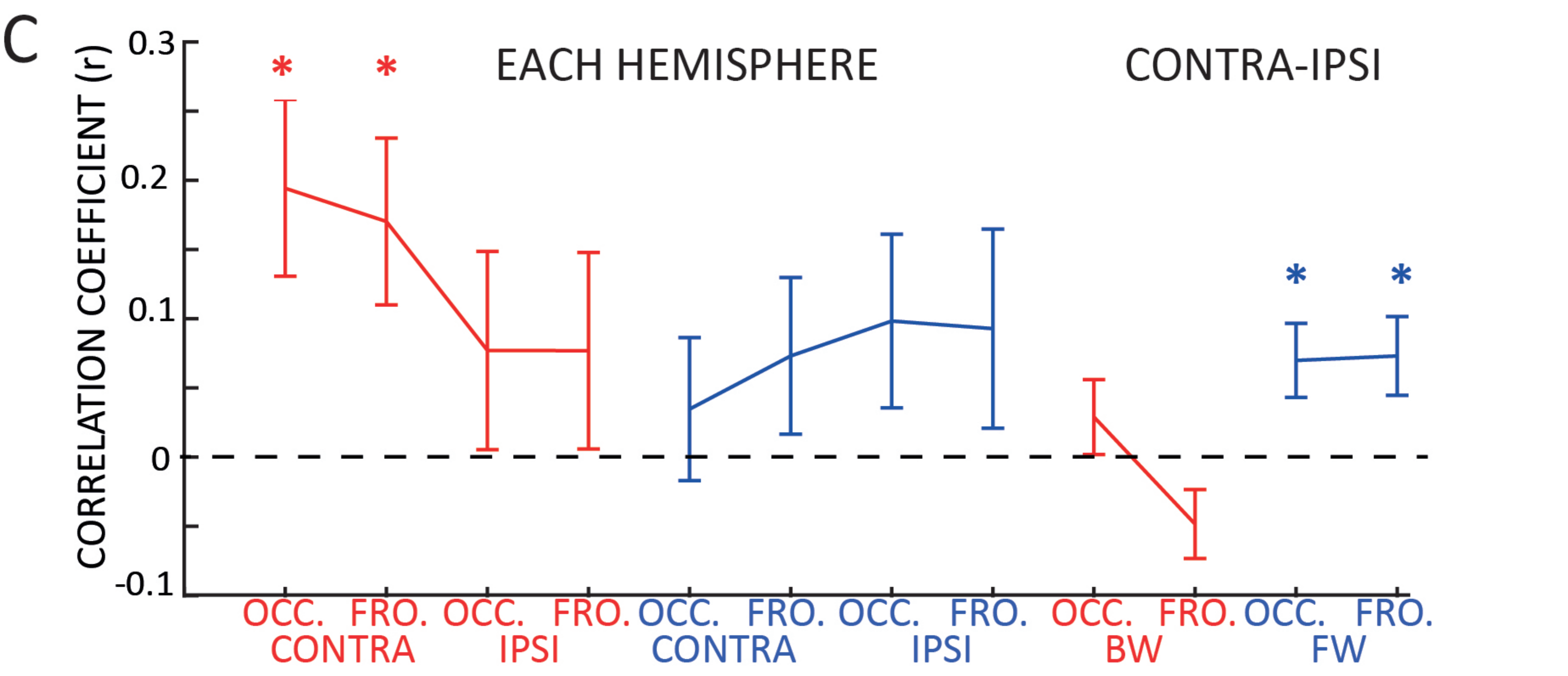
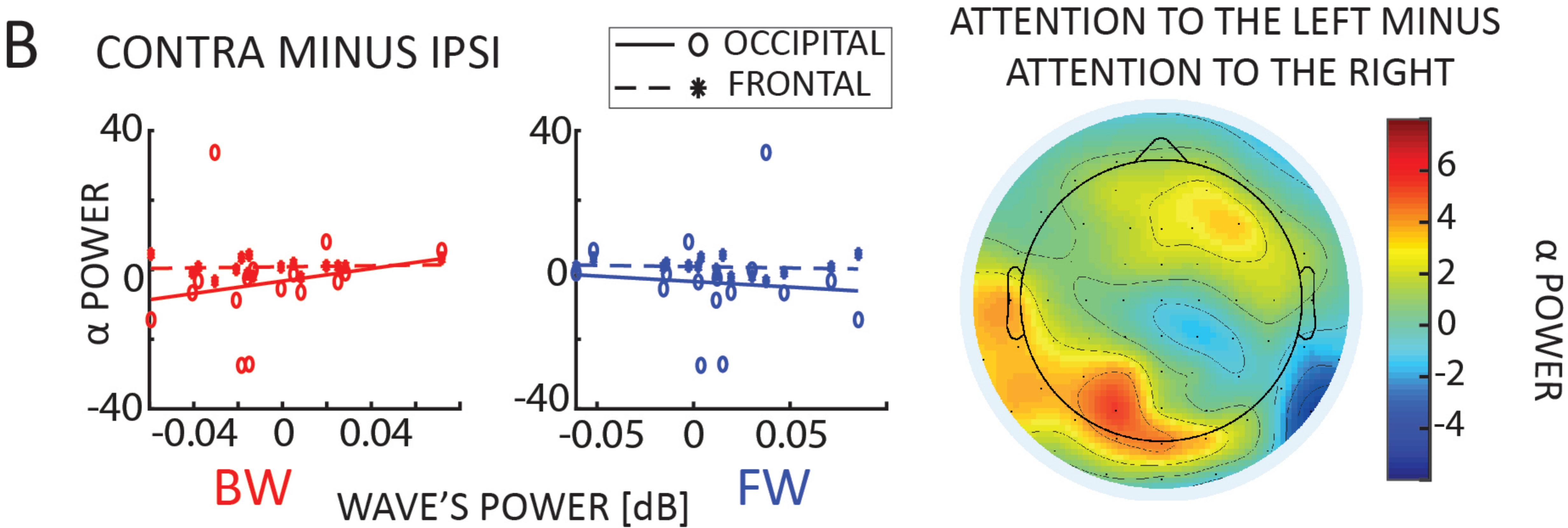
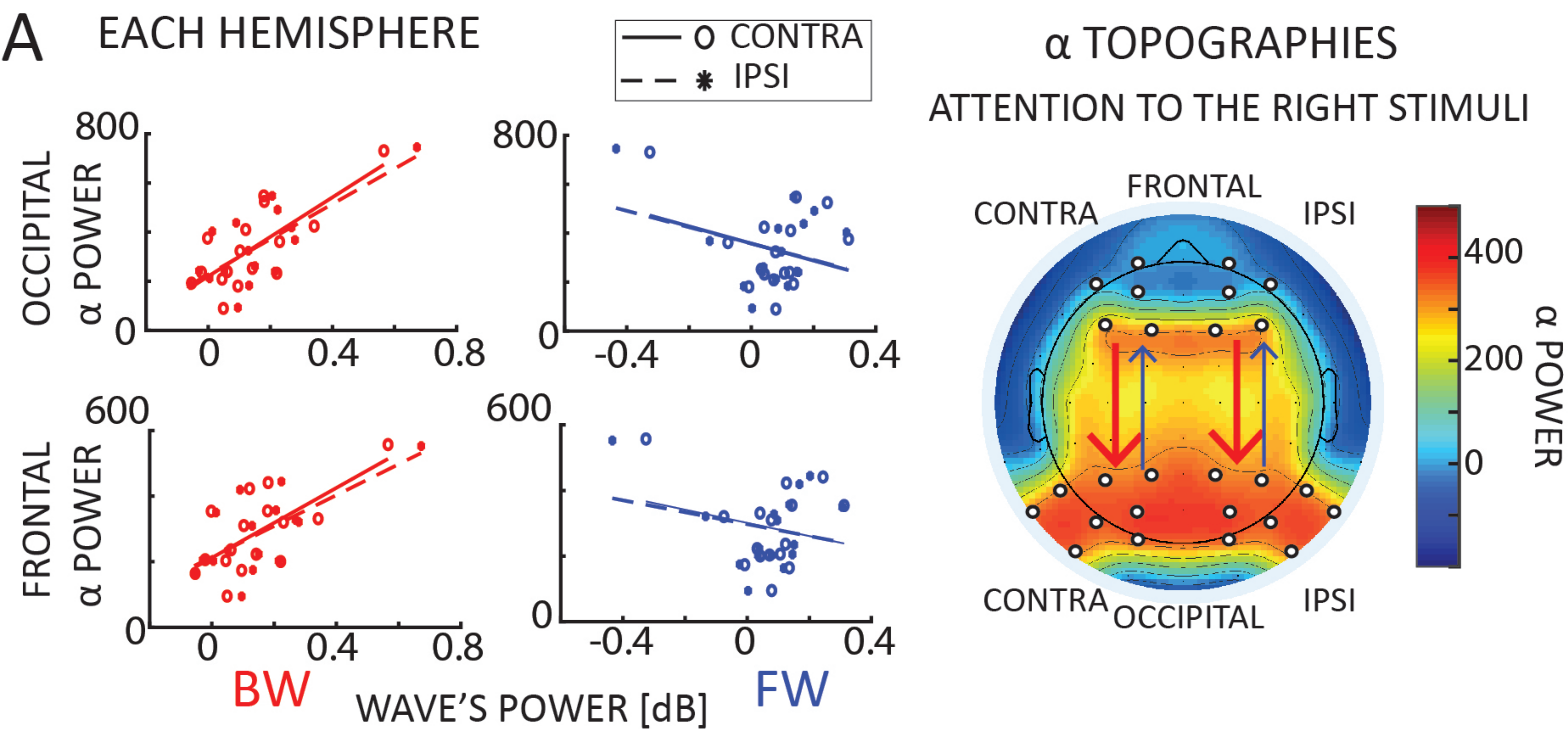


ATTENTION TO THE RIGHT

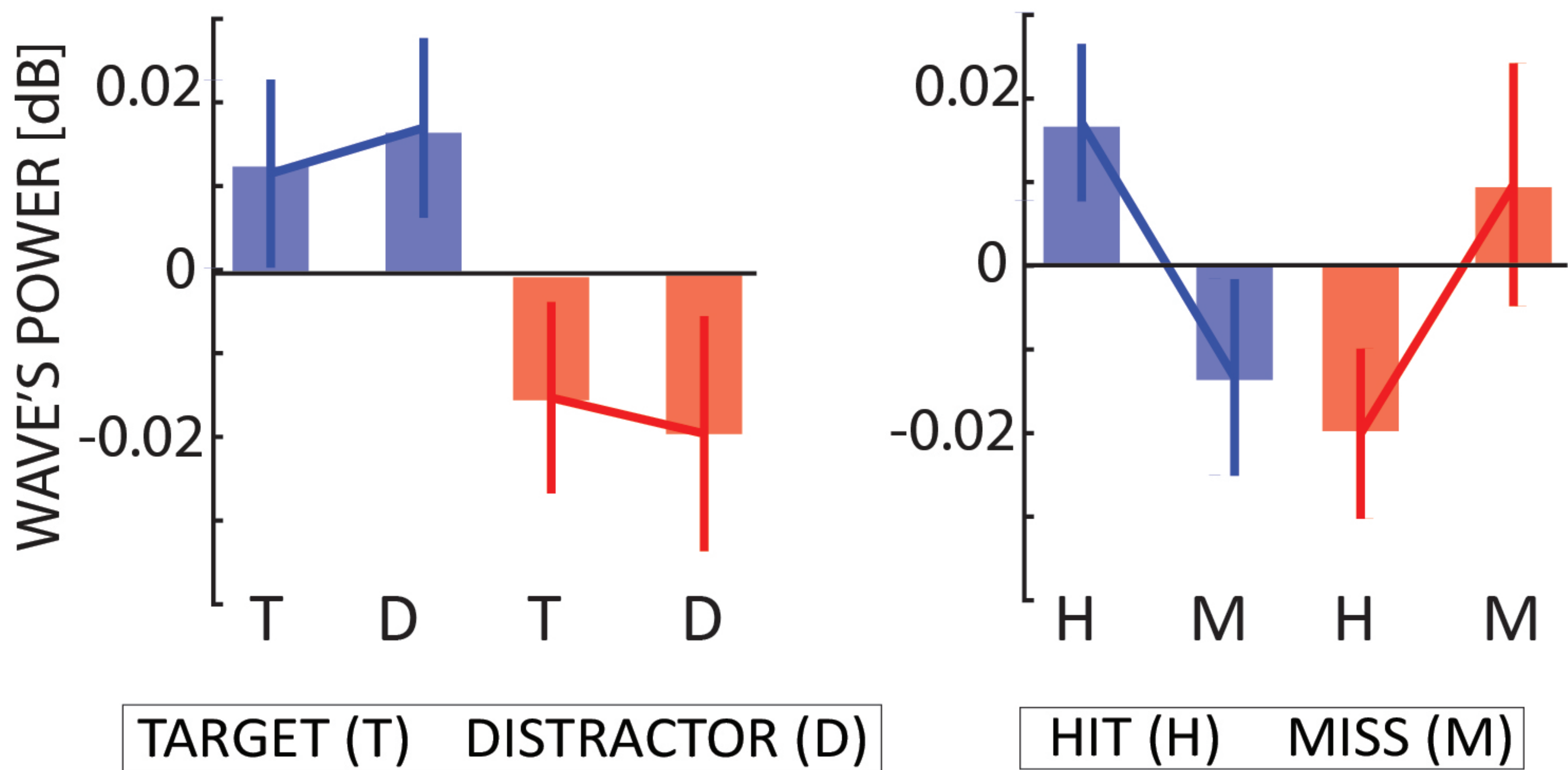


ATTENTION TO THE RIGHT





A FORWARD AND BACKWARD WAVES' AT STIMULUS ONSET
IN CONTRALATERAL ELECTRODES



B

FORWARD

BACKWARD

